nature aging

Article

https://doi.org/10.1038/s43587-022-00341-6

Exposure to negative socio-emotional events induces sustained alteration of resting-state brain networks in older adults

Received: 5 November 2020

Accepted: 29 November 2022

Published online: 12 January 2023

Check for updates

Sebastian Baez-Lugo[1,2] ✉, Yacila I. Deza-Araujo[1,2], Christel Maradan[2], Fabienne Collette[3], Antoine Lutz[4], Natalie L. Marchant[5], Gaël Chételat[6], Patrik Vuilleumier[1,2] ✉, Olga Klimecki[1,7] ✉ & Medit-Ageing Research Group*

Basic emotional functions seem well preserved in older adults. However, their reactivity to and recovery from socially negative events remain poorly characterized. To address this, we designed a 'task–rest' paradigm in which 182 participants from two independent experiments underwent functional magnetic resonance imaging while exposed to socio-emotional videos. Experiment 1 ($N = 55$) validated the task in young and older participants and unveiled age-dependent effects on brain activity and connectivity that predominated in resting periods after (rather than during) negative social scenes. Crucially, emotional elicitation potentiated subsequent resting-state connectivity between default mode network and amygdala exclusively in older adults. Experiment 2 replicated these results in a large older adult cohort ($N = 127$) and additionally showed that emotion-driven changes in posterior default mode network–amygdala connectivity were associated with anxiety, rumination and negative thoughts. These findings uncover the neural dynamics of empathy-related functions in older adults and help understand its relationship to poor social stress recovery.

Aging entails many changes in bodily and mental health. Although physical performances and cognitive abilities decline, emotional functions seem maintained or even enhanced in older relative to younger adults[1,2]. Older adults regulate their emotional states well, a crucial capacity for affective well-being and healthy aging[3]. Unlike younger adults, they often prioritize social and emotional interactions over other goals and show a 'positivity bias' in emotion perception[4]. In contrast, maladaptive emotional reactivity and impaired emotion regulation are related to psychopathologies such as anxiety, depression, worry and rumination throughout the lifespan[5,6], including in aging[7]. Maladaptive affective styles may represent an important risk factor for dementia[8–10], a major health burden[11]. However, the neural substrates underpinning proficient socio-affective processing and emotional resilience in older adults remain unresolved.

Maladaptive affective style may lead to 'emotional inertia', whereby emotions tend to carry over from one moment to the next[12]. Emotional inertia may reflect unsuccessful recovery mechanisms following affective events and low resilience to stress, associated with higher depression risks[13,14] and higher trait anxiety and rumination tendencies[15]. Recent neuroimaging studies investigated emotional inertia using 'task–rest' paradigms[16–22] where brain activity is probed not only during active stimulus processing but also in spontaneous post-task

[1]Swiss Center for Affective Sciences, University of Geneva, Geneva, Switzerland. [2]Laboratory for Behavioral Neurology and Imaging of Cognition, Department of Neuroscience, Medical School, University of Geneva, Geneva, Switzerland. [3]GIGA-CRC In Vivo Imaging Research Unit, University of Liège, Liège, Belgium. [4]EDUWELL team, Lyon Neuroscience Research Centre (INSERM U1028, CNRS UMR5292, Lyon 1 University), Lyon, France. [5]Division of Psychiatry, University College London, London, UK. [6]Université Normandie, Inserm, Université de Caen-Normandie, Inserm UMR-S U1237, GIP Cyceron, Caen, France. [7]Deutsches Zentrum für Neurodegenerative Erkrankungen, Dresden, Germany. *A list of authors and their affiliations appears at the end of the paper. ✉e-mail: sebastian.baezlugo@unige.ch; patrik.vuilleumier@unige.ch; olga.klimecki@unige.ch

resting periods while the brain returns to homeostatic balance[23,24]. Positive or negative emotions evoked by images or videos were found to induce lasting carryover effects on activity and/or connectivity of brain networks during subsequent rest[17,21]. These effects may occur at different timescales (from seconds[25] to minutes[20]), following different tasks (from passive viewing to active regulation of emotions[16]) and across different conditions of emotional valence and intensity[18,19].

At the brain level, emotion carryover effects generally affect the functional dynamics of the default mode network (DMN) in the form of either increased[19,25] or decreased[17,18] activity patterns in regions comprising the medial prefrontal cortex (MPFC), posterior cingulate cortex (PCC), precuneus and inferior parietal cortex. These DMN regions are usually active when individuals are free to let their minds wander in undisturbed conditions[26]. Similar effects have been observed in the insula and amygdala[17]—two regions involved in emotional and social processing[27–29]. Slower recovery of amygdala activity after emotional videos correlated with higher anxiety and ruminations[15]. Subcortical limbic regions in amygdala and striatum also display sustained changes in their functional connectivity with cortical areas in medial PFC and PCC during rest after negative emotions[17] and reward[21]. These findings converge with studies showing that disturbances in functional connectivity of the amygdala with medial parts of the DMN at rest are associated with anxiety (for example, decreased connectivity with MPFC[30]) and mood disorders (for example, increased connectivity with PCC[31]). These long-lasting carryover effects of emotions on activity and connectivity of limbic networks may provide an important neural marker of emotional regulation style and affective resilience.

However, previous work concerning emotional carryover focused on young healthy participants. It remains unknown whether emotional inertia occurs in older adults, how it is modified given the well-known 'positivity effect' observed in this population relative to younger adults[1,32], and how age impacts DMN functional dynamics in affective contexts. Unlike young adults, older people fail to deactivate the DMN during externally directed cognitive tasks[33] and show increased DMN connectivity with cognitive-related prefrontal regions[34]. Yet, little is known about how aging affects DMN responses to emotion and how this relates to other cognitive or socio-affective abilities.

In addition, individual differences in empathy may strongly influence responses to negative socio-affective events[15,17], and possibly recovery from these events[20]. Because social competencies are relatively preserved in older adults[2], socially significant emotional events offer an optimal window to probe affective reactivity and recovery in this population. Empathy is only scarcely studied in older people[2,35–37], with some evidence for a decline of cognitive empathy but intact or even enhanced affective empathy and altruistic behaviors[2,37,38]. However, brain responses to seeing others' pain are reduced in anterior insula (AI) and anterior cingulate cortex (ACC)[35], two regions implicated in pain processing, negative affect and salience detection[28,39]. In contrast, empathy-related responses may increase in superior temporal sulcus (STS) and temporoparietal junction (TPJ)[36], brain regions frequently associated with the Theory of Mind and perspective taking[40]. Yet, despite the importance of social interactions and emotional resilience for healthy aging[41,42], neural substrates underlying the recovery from negative events, as well as their link with empathic skills, personality and psycho-affective traits, have not been investigated during aging.

To address these issues, we designed a 'task–rest' paradigm combining two lines of research: short (10–18 s) empathy-inducing videos from the socio-affective video task (SoVT)[43] were shown interspersed with rest periods of 90 s (similarly to Eryilmaz and colleagues[17]) while participants underwent functional magnetic resonance imaging (fMRI) of brain activity (Extended Data Fig. 1). Videos consisted of short silent scenes depicting suffering people (high emotion, HE) or people in everyday life situations (low emotion, LE). By adding resting-state periods after blocks of videos of each kind, our paradigm allowed probing how the aging brain reacts both during and after exposure to emotionally challenging social information.

Using this paradigm, we conducted two experiments to assess emotion-related carryover effects in large samples of healthy older and young participants ($N = 182$). First (experiment 1), we compared the neural substrates of emotional recovery between old ($n = 26$; mean age, 68.7 years) and young ($n = 29$; mean age, 24.5 years) participants, allowing us to validate our paradigm and identify age-related effects. Next (experiment 2), we replicated this experiment in a large sample of older adults ($n = 127$; mean age, 68.8 years) and specifically investigated whether emotional inertia in brain networks is modulated by empathy and individual traits relevant for healthy aging, including rumination and anxiety. We hypothesized that exposure to others' suffering (relative to neutral social situations) should: (1) engage brain regions implicated in emotional saliency and empathy (that is, insula and anterior medial cingulate cortex (aMCC)), but with lower responses in older than young adults;[35] (2) induce subsequent carryover in functional connectivity at rest between emotion-related regions and DMN, with differential age-dependent patterns; and (3) unveil neural substrates of emotional inertia reflecting individual variability in anxiety, ruminative thinking and negative emotions, and thus point to functional biomarkers of affective risk factors for pathological aging[8–10]. We also expected to (4) observe a 'positivity effect' as often reported in older adults[4], characterized by higher positive affect during the task in older compared to younger adults, and elucidate any relationship to affective empathy.

Results

Participant characteristics

Demographical data, psycho-affective traits, cognitive abilities and socio-emotional questionnaires are reported in Table 1 and Fig. 1.

Behavioral responses in the SoVT–rest task and age effects

Subjective ratings (empathy, positive and negative affect) showed that HE videos induced higher levels of negative affect, lower positive affect and higher empathy scores than LE videos in both younger and older participants in both experiments, validating successful emotional elicitation with the SoVT–rest task (Fig. 2a). All video sets elicited similar emotional responses (Supplementary Fig. 1) and differences between HE and LE were not affected by sex (Supplementary Fig. 6).

In experiment 1, we also examined age-dependent differences in ratings. Independent analysis of variance (ANOVA) showed main effects of age on empathy ($F(1,53) = 10.8$, $P = 0.002$) and positive affect ($F(1,53) = 24$, $P < 0.001$), not on negative affect ($F(1,53) = 1.01$, $P = 0.3$). Follow-up two-sample t-tests revealed higher empathy levels in older than younger adults only for LE videos ($t_{51.5} = 4.45$, $P < 0.001$, $d = 1.19$, two-tailed) as well as higher positive emotions for both HE ($t_{36.5} = 4.63$, $P < 0.001$, $d = 1.29$, two-tailed) and LE ($t_{50.1} = 3.68$, $P < 0.001$, $d = 0.98$, two-tailed) videos. Our two older samples (experiments 1 and 2) did not differ in any of the scores (all $t \leq 1.8$, $P \geq 0.07$; Fig. 2a) except for even higher empathy ratings for LE videos in older adults from experiment 2 than those from experiment 1 ($t_{36} = 2.20$, $P = 0.03$, $d = 0.47$, two-tailed).

We further tested for age-dependent effects within each age group separately (young and older) by computing Spearman correlations between age (as a continuous variable) and ratings (collapsing both older samples from experiments 1 and 2). Age correlated negatively with negative affect (rho = −0.2, false discovery rate (FDR)-adjusted P value (P_{FDR}) = 0.03) and positively with positive affect (rho = 0.25, $P_{FDR} = 0.006$) during HE video for older individuals but not younger adults. In addition, age correlated positively with empathy for LE videos in the young adults (rho = 0.44, $P_{FDR} = 0.03$) but not older adults (Fig. 2b). The same results were obtained after excluding eight older adults who reported 'moderate' depression levels (Geriatric Depression Scale, GDS > 5; ref. 44; Supplementary Table 5). These participants were therefore kept for subsequent analyses.

To test whether empathy influenced positive and negative affect, we computed Spearman correlations between these rating scales. For both younger and older adults, higher empathy predicted increased

https://doi.org/10.1038/s43587-022-00341-6

Table 1 | Participant characteristics

		Experiment 1			Experiment 2
		Mean (s.d.) *N*=55		*P* value for between-group differences[a]	Mean (s.d.)
		YA group (*n*=29)	OA group (*n*=26)		OA group *N*=127
Demographics					
Sex		14 females	13 females		79 females
Age (years)		24.5 (2.67)	68.7 (3.89)		68.8 (3.65)
Education (number of years)		18.4 (1.72)	16.1 (3.4)	0.002	13.21 (3.1)
Psycho-affective traits and cognitive functions					
State-Trait Anxiety Inventory	Trait	39.8 (8.31)	36 (7.31)	0.08	34.57 (7.12)
Rumination Response Scale[b]	Total	43.5 (10)	36.5 (9.01)	0.008	35.67 (8.55)
	Reflection	11.3 (3.67)	8.77 (3.52)	0.01	8.93 (3.23)
	Brooding	8.97 (2.64)	8.69 (2.41)	0.69	8.06 (2.28)
Interpersonal Reactivity Index	Distress	12 (4.3)	9.62 (5.12)	0.07	10.18 (5.27)
	Empathic concern	22.1 (3.14)	20.8 (4.24)	0.19	19.76 (4.18)
	Perspective taking	21.3 (3.71)	17.3 (3.42)	<0.001	17.50 (3.56)
	Fantasy	19.1(4.05)	15.8 (4.08)	0.004	14.35 (4.75)
Emotion regulation abilities	Reappraisal	30.5 (7.11)	29.2 (3.95)	0.4	29.61 (5.79)
	Suppression	12.6 (5.48)	14.8 (4.34)	0.09	16.54 (5.19)
Beck Depression Inventory	Global	5.34 (3.73)			
Geriatric Depression Scale	Global		1.92 (2.3)		1.32 (1.78)

YAs, younger adults; OAs, older adults; *N*, number of total participants in each experiment; *n*, number of participants in each subgroup. [a]Between-group differences were assessed using *t*-tests; statistical significance was set to $P<0.05$. [b]Values were computed on *n*=126 participants (data are missing for one participant).

negative affect during HE videos (YOUNG: rho = 0.86, $P_{FDR} < 0.001$; OLD: rho = 0.63, $P_{FDR} < 0.001$) and higher positive affect during LE videos (YOUNG: rho = 0.75, $P_{FDR} < 0.001$; OLD: rho = 0.65, $P_{FDR} < 0.001$). Interestingly, during HE videos, empathy correlated negatively with positive affect for older (rho = −0.35, $P_{FDR} < 0.001$) but not younger (rho = 0.27, $P_{FDR} = 0.18$) adults; whereas during LE videos, empathy correlated positively with negative affect for the younger (rho = 0.63, $P_{FDR} < 0.001$) but not the older (rho = 0.13, $P_{FDR} = 0.14$) adults (Fig. 2c).

Brain activity during the SoVT–rest task

Age-related differences in response to others' suffering. After confirming differential brain activity during videos and rest periods (Supplementary Fig. 2), we determined the effect of the emotional condition in each age group, as well as age-related differences (experiment 1). In both groups, comparing HE and LE videos (voxel-wise $P < 0.05$ using family-wise error (FWE) correction; and $P < 0.001$ uncorrected, $k = 20$) demonstrated increases in left TPJ, right inferior-frontal gyrus (IFG), as well as temporal and occipital cortices (Fig. 3a and Supplementary Table 3a). Older adults showed larger activations in PCC and dorsomedial prefrontal cortex (dMPFC), whereas younger adults showed additional increases in AI and periaqueductal gray (PAG) (Fig. 3a). A direct between-group comparison (2 × 2 ANOVA) revealed stronger cortical responses for the older adults in bilateral angular gyrus (TPJ/IPL) and dorsolateral PFC. The young adults showed stronger activation in subcortical areas of ventral striatum and PAG, as well as in sensory areas in parietal and occipitotemporal cortices (Fig. 3b).

These activation patterns across both experiments overlap with brain networks classically associated with empathy[28,39], compassion[43,45,46], as well as cognitive and affective theory of mind[40,47].

Carryover effects during post-emotion rest periods. To test for carryover effects of emotional videos on brain activity[17], we compared rest periods after HE videos to those after LE videos. In experiment 1, this contrast (voxel-wise $P < 0.001$ uncorrected, $k = 20$) revealed greater activations, mostly in the older group, involving MPFC, left AI, right IFG, several temporoparietal cortices and right hippocampus (Fig. 4a and Supplementary Table 3a). The younger adults showed more limited increases, predominating in MCC. A direct between-group comparison (2 × 2 ANOVA) confirmed that older adults engaged these regions (AI, IFG and dMPFC) more strongly, with further significant effects in left MTG and left amygdala, whereas the younger adults showed higher activity in left hippocampus and precentral motor regions (Fig. 4b and Supplementary Table 3a).

In experiment 2, similar regions were found, surviving a more stringent statistical threshold and replicating our results in older adults from experiment 1. Post-HE > post-LE rest periods (voxel-wise $P < 0.05$ FWE corrected) disclosed higher activity among midline DMN nodes (ACC/dMPFC, and precuneus/PCC), as well as in the right amygdala and ventral right anterior insula (Fig. 4c and Supplementary Table 3b).

The larger sample size in experiment 2 allowed us to conduct additional analyses to assess whether carryover effects at rest directly resulted from higher activity in the same regions during videos periods. We identified voxels with the strongest emotional response (HE > LE) across the two periods (videos and rest) by applying an inclusive mask from one contrast (for example, videos: HE > LE) to the other contrast (rest: post-HE > post-LE), with a strict threshold for both ($P < 0.00001$). This overlap analysis identified brain areas showing persistent emotion-related increases across both video and rest conditions (Fig. 4c). Results highlighted a restricted set of regions, mainly dMPFC and PCC, where greater emotional activation during videos was followed by emotional carryover effects during rest after videos (Fig. 4e,f). Other regions activated during emotional videos did not display differential carryover effects in subsequent rest, including visual cortex and MCC (Fig. 4d). Interestingly the right amygdala and the right ventral AI did not show significant differences for HE > LE during videos but were robustly activated in post-HE > post-LE rest periods (Fig. 4g,h). Figure 4

https://doi.org/10.1038/s43587-022-00341-6

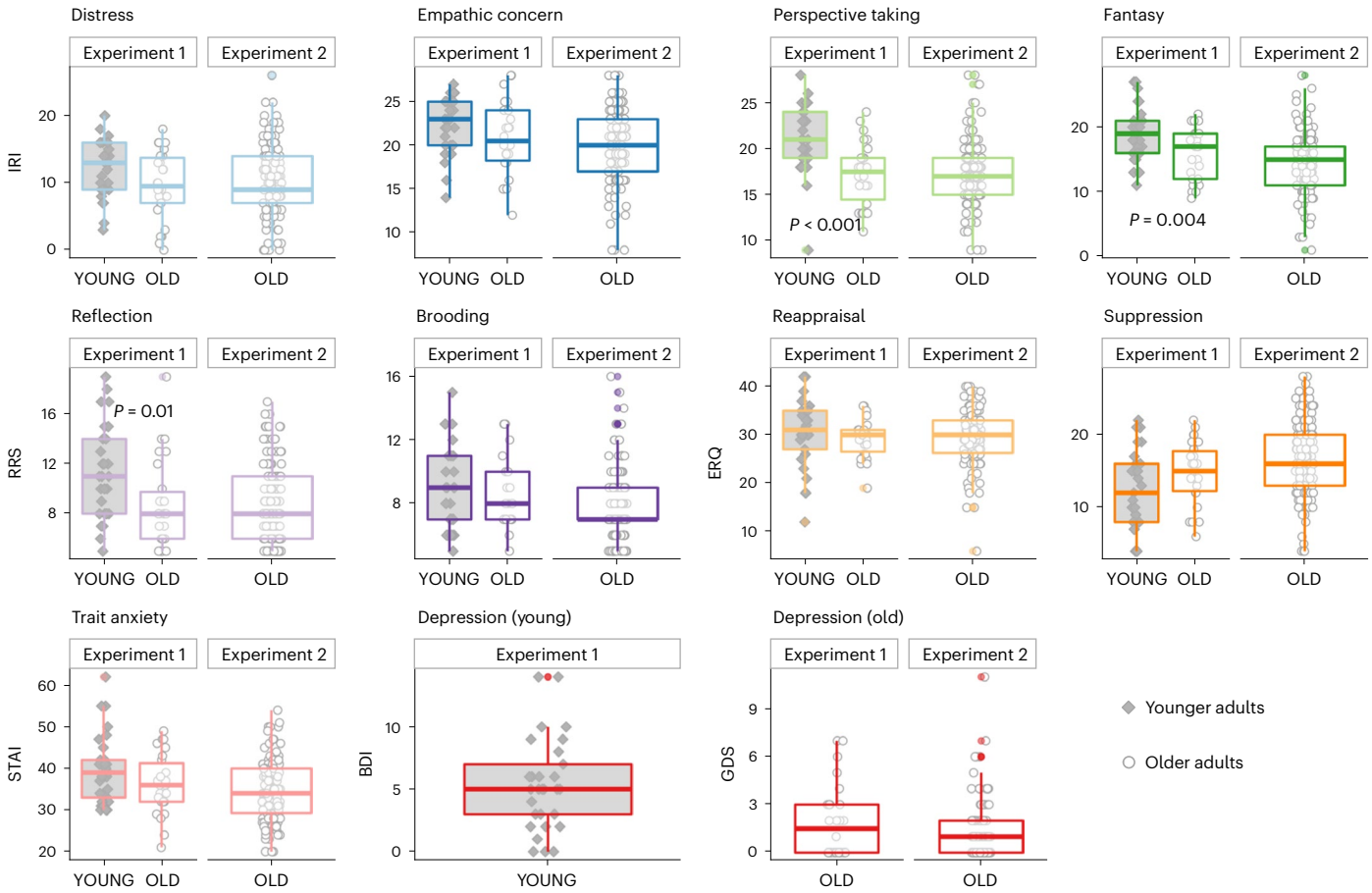

Fig. 1 | Participants' characteristics in terms of psycho-affective traits and socio-emotional competencies for both experiment 1 and experiment 2. Age-related differences (experiment 1) were tested with *t*-tests (two-sided), and *P* values for significant results are displayed. Older versus younger participants (experiment 1) did not differ in trait anxiety, affective empathy and emotion regulation scores. However, older adults reported lower scores of cognitive empathy in the perspective taking ($t_{53} = 4.2$, $P < 0.001$, d = 1.13, two-tailed) and the fantasy subscales of the IRI ($t_{52.3} = 3$, $P = 0.004$, d = 0.81, two-tailed). Older adults also had lower scores in reflective rumination ($t_{52.7} = 2.62$, $P = 0.01$, d = 0.7, two-tailed). The two independent samples of older adults, that is, experiment 1 ($n = 29$ younger and $n = 26$ older adults) and experiment 2 ($N = 127$ older adults), did not differ in any of the scores (all $t \leq 1.6$, all $P \geq 0.09$, two-tailed). Gray diamonds denote younger adults; white dots denote older adults. GDS (for older adults only); BDI, Beck Depression Inventory (for younger adults only); STAI, State-Trait Anxiety Inventory; ERQ, Emotion Regulation Questionnaire (See Table 1 for further statistical details).

illustrates this dissociation by plotting brain activity (contrasts estimates) over successive time bins of the video and rest periods across emotion conditions (Fig. 4d–h).

Differential effect on network connectivity in older adults. To further assess emotional carryover in brain activity dynamics, we examined changes in functional connectivity within and between the DMN, the empathy network, and the bilateral amygdala, during post-HE versus post-LE rest periods. Connectivity was computed using Pearson correlation matrices for each condition and each participant, and then compared between post-HE and post-LE using permutation tests (Methods and Extended Data Fig. 2). Consistent with functionally coherent activity within each network, we observed general patterns of intra-network connectivity (Empa-Empa, Amy-Amy, DMN-DMN) for both conditions and both age groups (Supplementary Fig. 3)

In experiment 1, differences in functional connections of the DMN were found only in older adults: relative to post-LE rest, post-HE periods rest showed stronger coupling of PCC with right amygdala ($t = 2.52$, $P = 0.008$, $Z = 2.4$, one-tailed) and left amygdala ($t = 2.1$, $P = 0.02$, $Z = 1.97$, one-tailed), as well as between anterior medial prefrontal cortex (aMPFC) and right amygdala ($t = 2.02$, $P = 0.03$, $Z = 1.95$, one-tailed), and between aMPFC and left amygdala ($t = 2.24$, $P = 0.02$, $Z = 2.04$, one-tailed; Fig. 5a). No such differences were found for young adults (Fig. 5a).

These age-related differences were confirmed by *t*-tests for each connectivity node between younger and older adults at rest (post-HE > post-LE). Compared to younger adults, the older adults showed enhanced connectivity between left amygdala and PCC ($t = 2.12$, $P = 0.03$, two-tailed), and between left amygdala and aMPFC ($t = 2.08$, $P = 0.04$, two-tailed; Fig. 5b).

Experiment 2 revealed similar patterns of increased connectivity in our larger group of older adults. Significant differences were observed for highly selective functional connections of the DMN with limbic areas: compared to post-LE rest, the post-HE rest periods induced stronger coupling between the PCC and right amygdala ($t = 1.82$, $P = 0.03$, $Z = 1.81$ one-tailed), as well as between the aMPFC and left insula ($t = 1.98$, $P = 0.02$, $Z = 2.02$ one-tailed). There was also higher coupling among the bilateral amygdala during post-HE versus post-LE rest periods (right with left, $t = 1.88$, $P = 0.02$, $Z = 1.95$ one-tailed; Fig. 5c). Further *t*-tests revealed that the increased functional coupling induced by emotional videos was stronger in r.AMYG–PCC than in other pairs of nodes engaging either the right amygdala or the PCC such as l.AI–PCC, r.AI–PCC and r.AMYG–aMPFC (Fig. 6a).

Neural emotional carryover and psycho-affective measures. Our fMRI connectivity analyses identified a selective impact of emotional videos on functional brain connectivity of the posterior DMN (PCC)

https://doi.org/10.1038/s43587-022-00341-6

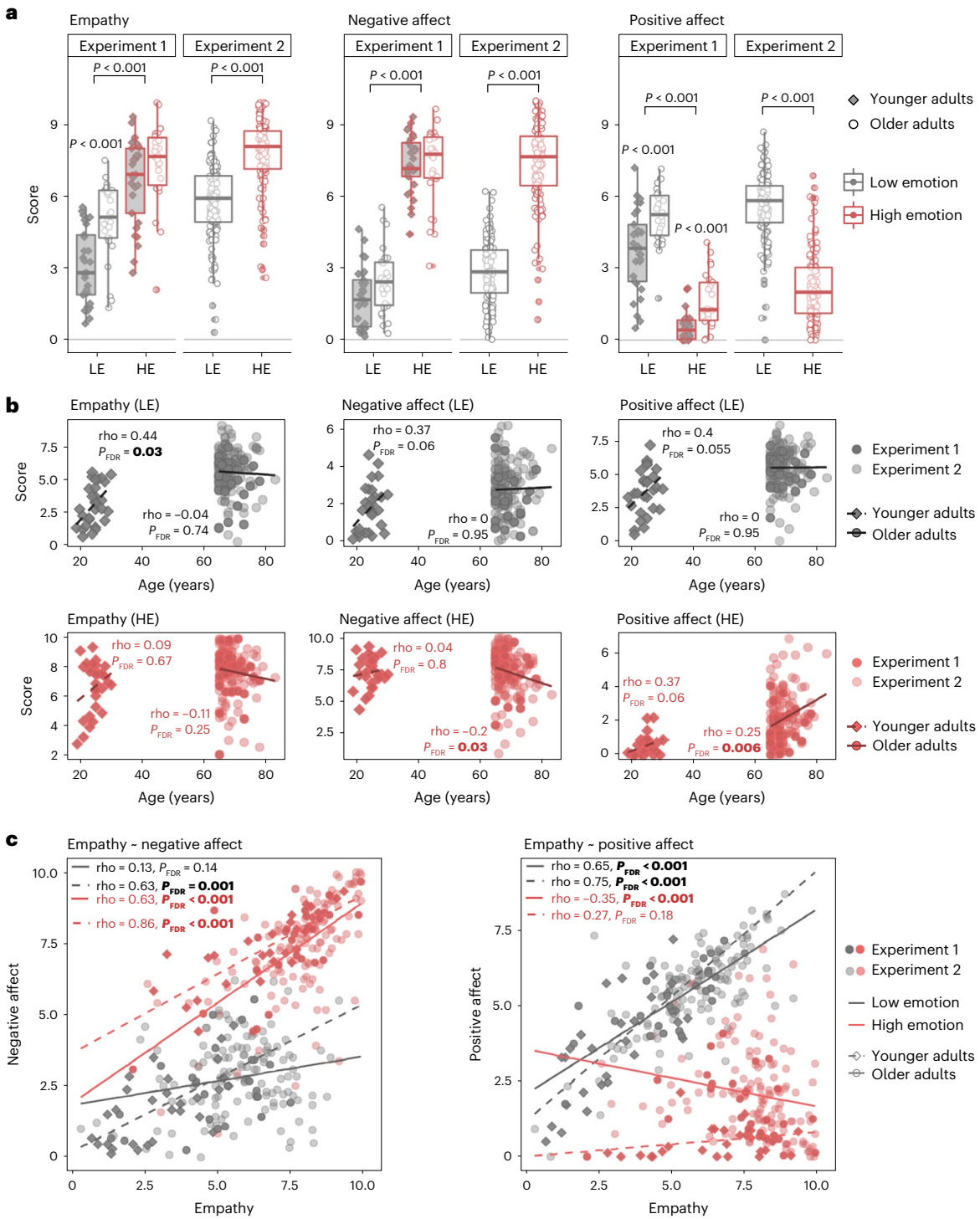

Fig. 2 | Empathy, positive affect, and negative affect during high and low emotion videos across experiments and age groups. a, Self-reported scores of empathy, positive affect and negative affect for HE and LE videos. HE and LE videos were compared using pairwise *t*-tests for each of these ratings. Results from experiment 1 were fully replicated in experiment 2. Participants reported higher levels of empathy (Exp 1: $t_{54} = 14.35$, $P < 0.001$, d = 1.67, two-tailed; Exp 2: $t_{126} = 14.5$, $P < 0.001$, d = 1.31, two-tailed), higher negative affect (Exp 1: $t_{54} = 23.35$, $P < 0.001$, d = 3.77, two-tailed; Exp 2: $t_{126} = 26.9$, $P < 0.001$, d = 2.89, two-tailed) and lower positive affect (Exp 1: $t_{54} = -16.85$, $P < 0.001$, d = −2.31, two-tailed; Exp 2: $t_{126} = -18.9$, $P < 0.001$, d = −2.31, two-tailed), when presented with HE as compared to LE videos. The box plots show the interquartile range (25th percentile, median and 75th percentile), the whiskers (indicating variability outside the interquartile range) and the individual data points. Significant differences between age groups or video conditions are marked by ***$P < 0.001$, uncorrected for multiple comparisons. **b**, Scatterplots illustrate Spearman correlations between age and scores of empathy, positive affect and negative affect. **c**, Scatterplots illustrate Spearman correlations between scores of empathy and affective ratings. For **b** and **c**, correlation coefficients were obtained using two-sided tests, and analyses were computed together; therefore, *P* values are corrected for multiple comparisons using the FDR method. For **b** and **c**, significant *P* values are marked in bold. Dots represent averaged values for each participant per condition; dots/solid lines indicate older adults, and diamonds/dashed lines indicate younger adults; $n_{Exp1} = 55$ (29 younger and 26 older adults), $n_{Exp2} = 127$ older adults. Red indicates HE videos; gray indicates LE videos.

https://doi.org/10.1038/s43587-022-00341-6

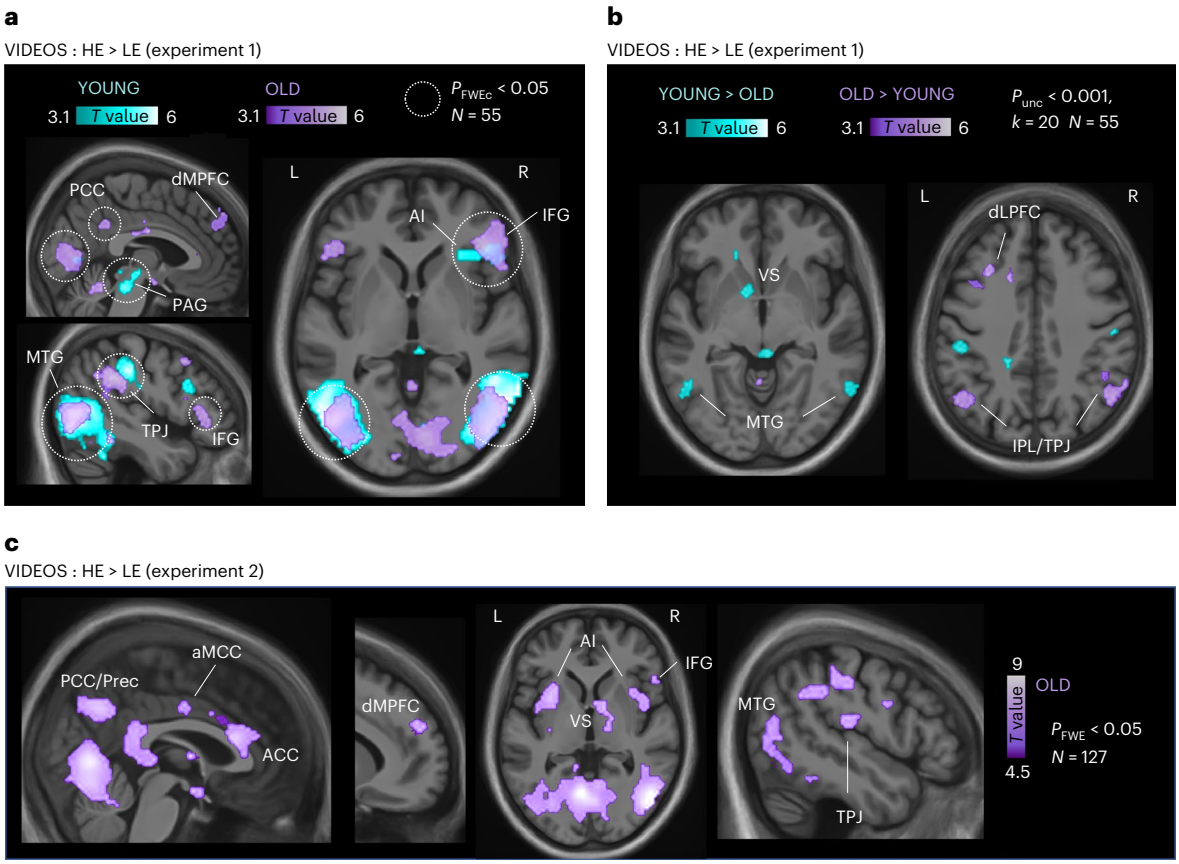

Fig. 3 | Brain regions with greater activation during high emotion videos compared to low emotion videos across experiments and age groups. **a**, Brain maps for younger ($n = 29$) and older ($n = 26$) adults in experiment 1. **b**, Between-age-groups difference in experiment 1. For display purposes, results are thresholded at uncorrected $P < 0.001$, with a minimum cluster size of ($k = 20$). Clusters surviving correction for multiple comparisons (P FWE < 0.05 at the cluster level) are surrounded in white-dotted circles. **c**, Brain maps for older adults ($N = 127$) in experiment 2. Results survived FWE correction at the voxel level ($P < 0.05$ FWE corrected). For **a**–**c**, t-statistics were obtained from the corresponding contrasts of interest (t-tests, one-sided). Overall, HE > LE videos activated regions previously reported as part of the Empathy Network (bilateral AI, aMCC), and regions in the Theory of Mind network (left TPJ; dMPFC) and the Compassion network (VS, ventral striatum)[46,50]. Full statistics on each cluster and related brain areas are in Supplementary Table 3a,b. Given the age-related positivity in affective ratings observed behaviorally in older adults (Fig. 2), we also computed regression analyses to examine whether whole-brain activity during emotional videos (HE–LE) was modulated by individual differences in self-reported positive affect scores, but this revealed no significant effects across experiments or age groups (Supplementary Fig. 7).

with the amygdala, replicated across two independent experiments carried out at different sites. These results provide a plausible neural mechanism underlying emotional inertia[12,17] that is specific to older adults and may thus offer a valuable biomarker of homeostatic emotion regulation processes in aging.

In experiment 2, we could further examine whether this connectivity pattern reflected individual differences in socio-emotional abilities and psycho-affective traits. We tested for a correlation between significant changes in connections between two regions of interest (ROIs; $Z > 1.64$ for difference post-HE versus post-LE rest) and scores on trait anxiety (STAI-trait), rumination (Rumination Response Scale, RRS) and empathy (Interpersonal Reactivity Index, IRI). This revealed a significant positive relationship between the magnitude of changes in r.AMYG–PCC connectivity (rest HE > rest LE) and individual levels of trait anxiety ($r = 0.21$, $P < 0.01$, two-tailed) and rumination (rho = 0.22, $P < 0.01$, two-tailed; Fig. 6b), but no correlation with empathy ($r = 0.1$, $P = 0.25$, two-tailed). On the other hand, the age-dependent positivity effect observed behaviorally in affective ratings (Fig. 2) was found not to be related to emotional carryover in brain connectivity patterns, for neither r.AMYG–PCC nor aMPFC–insula (Supplementary Fig. 8).

Neural emotional carryover and thought probes. Because rumination scores were positively associated with greater changes in functional coupling between r.AMYG and PCC during post-emotion rest (HE > LE), we reasoned that some participants (that is, with higher ruminative tendencies) may hold more negative affect-related content in their thoughts during rest periods after emotional videos. This was directly tested in experiment 2 by using an explicit thought probe given after different rest periods (Extended Data Fig. 1b).

Behavioral results (Methods) showed more frequent reports of negative (54%) than non-negative (28%) thoughts in response to probes after emotional rest periods (X^2 (1, $N = 109$) = 45.88, $P < 0.001$, two-tailed). Conversely, negative thoughts were less frequent (37%) than non-negative (45%) thoughts after LE video (X^2 (1, $N = 110$) = 51.59, $P < 0.001$, two-tailed; Supplementary Table 4 and Fig. 6c).

We then compared the r.AMYG–PCC connectivity between a subgroup of participants who reported negative content in spontaneous thoughts in response to the probe (present) versus those who did not (absent), for both the HE and LE conditions. A non-parametric permutation analysis was applied where the r.AMYG–PCC connectivity difference between these two subgroups was compared to a null distribution built by permuting labels 5,000 times. As hypothesized, those 54% of participants reporting negative thought contents (versus 28% not reporting) showed increased r.AMYG–PCC connectivity during the rest periods after HE videos (observed difference = 0.08; $P = 0.02$, one-tailed). The same difference between the two subgroups during

https://doi.org/10.1038/s43587-022-00341-6

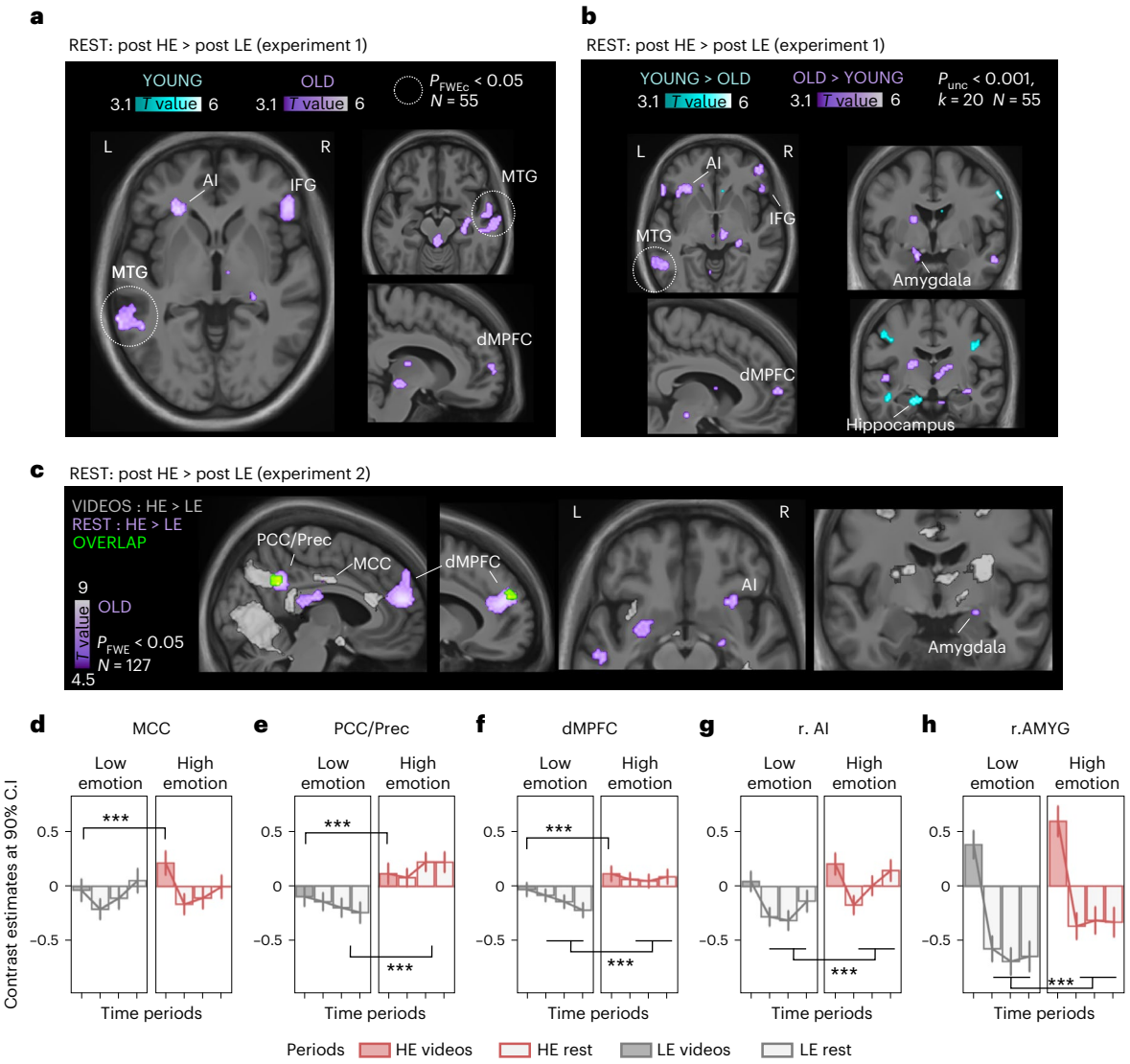

Fig. 4 | Carryover effects on brain activity at rest subsequent to high (post-HE) versus low emotion (post-LE) videos. a, Brain maps for younger ($n = 29$, blue clusters) and older adults ($n = 26$, violet clusters) in experiment 1. **b**, Direct comparisons of brain maps representing significant age-related differences in experiment 1, with threshold uncorrected $P < 0.001$ and minimum cluster size $k = 20$. Clusters surviving correction for multiple comparison (P FWE < 0.05 at the cluster level) are surrounded in white-dotted circles. **c**, Brain maps for older adults ($N = 127$) in experiment 2. Violet clusters show significant increases in post-HE > post-LE rest periods. Green clusters show the overlap of these activations with emotional responses to HE > LE videos (gray). Results are thresholded at $P < 0.05$ corrected for multiple comparisons using FWE correction at the voxel level. **d**–**h**, Magnitude and time course of brain activity (parameter estimates) for relevant regions during the different task periods in older adults from experiment 2. **d**, Example of a region (in MCC) responding to HE versus LE videos, but showing no significant difference during rest after HE versus LE videos. **e**,**f**, Example of regions (PCC/Prec and dMPFC) responding to HE > LE videos and showing significant carryover with sustained activity during subsequent rest. **g**,**h**, The r.AMYG and the right ventral AI did not reliably respond to HE versus LE videos but showed significant increases in activations during post-HE rest. Pink and gray lines track activity time courses during HE and LE conditions, respectively. Pink and gray bars indicate activity during videos (three in each block, ~45 s), and white bars indicate activity during subsequent rest (3 bins of 30 s). ***$P < 0.05$ FWE corrected. t-statistics were obtained from the corresponding contrasts of interest (t-tests, one-sided). Data for younger adults are not plotted given the lack of significant increases in brain activity at rest in this group (see **a**). Prec, precuneus; MTG, middle temporal gyrus; Hipp, hippocampus.

rest periods after LE videos showed only a trend (observed difference = 0.06; $P = 0.07$, one-tailed; Fig. 6c). These findings further unveil a direct relation between r.AMYG and PCC connectivity changes after negative emotions and individual reactivity to aversive or stressful socio-emotional stimuli.

Discussion

Neural markers of emotional resilience and empathy in aging are increasingly recognized as important protective factors against mental illness and cognitive decline in this population[48]. Here we investigated both reactivity and recovery of brain networks to negative socio-affective situations (that is, during and after videos) in two independent experiments, including a large number of younger and older adults ($N = 182$).

Age-related behavioral characteristics

Older adults in experiments 1 and 2 did not differ in demographic or questionnaire data assessing affective or cognitive traits. However, they exhibited lower scores than younger adults in cognitive-related processes, including reflective rumination and cognitive empathy. This

https://doi.org/10.1038/s43587-022-00341-6

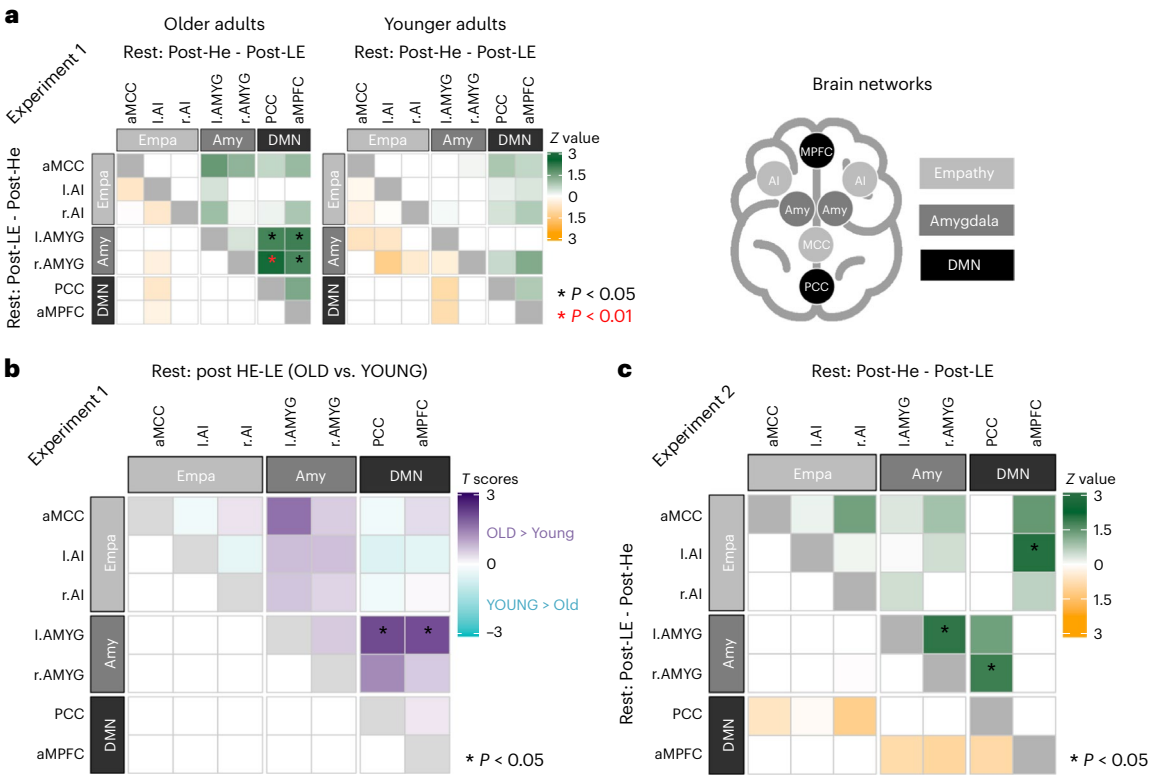

Fig. 5 | Functional connectivity between pairs of regions of interest for the different rest conditions in experiment 1 and experiment 2. a, Correlation matrices computed on the difference between the two rest conditions, showing post-emotion increases (green) and decreases (orange) in functional connectivity (FC) between regions, for each age group in experiment 1 ($N = 55$). Left and right halves of the matrix with respect to the diagonal depict values for opposite contrasts (upper part, post-HE > post-LE rest; lower part, post-LE > post-HE rest). Significant emotion effects ($Z > 1.64$) are marked by an asterisk (*$P < 0.05$, one-tailed). **b**, Age-related differences between emotion effects on FC (old versus young, two-sample *t*-tests) showed increases predominating in older (violet) or younger (blue) adults. Significant differences were observed only for older relative to younger adults (*$P < 0.05$, two-tailed, uncorrected). **c**, Correlation matrix showing significant differences in FC between rest conditions in older adults ($N = 127$) from experiment 2. For **a** and **c**, differences between correlation matrices (post-HE versus post-LE rest) were determined by non-parametric permutation statistics (Methods and Extended data Fig. 2), with a significance threshold of $Z > 1.64$ (equivalent to $P < 0.05$, one-tailed, given the observed increases without decreases in general linear model (GLM) analysis, uncorrected). The upper-right schematic illustrates a priori selected ROIs for this analysis, including nodes from the DMN (aMPFC), empathy network (Empa, left and right AI; MCC) and bilateral amygdalae (Amy, left and right AMYG).

accords with previous work showing a decline of cognitive abilities in aging, including cognitive components of social functions[2], while socio-affective abilities may remain stable. Indeed, measures of affect and empathy showed preserved patterns in older adults, extending previous findings in younger adults[43]. Seeing videos of others' suffering induced higher levels of negative affect, lower positive affect and higher empathy scores than mundane scenes of daily life, regardless of age group.

Nonetheless, age differences were observed, with older adults reporting more positive emotions for both LE and HE videos. Moreover, the older the age, the lower the negative and the higher the positive emotions were rated when watching videos of suffering (Fig. 2b). This relationship between age and affect was not present for young participants. These results confirm a 'positivity effect' in older relative to younger adults[4], which may reflect a motivation to upregulate positive and downregulate negative information[4]. In contrast, young and older adults reported similar levels of negative affect in response to videos. This suggests that the positivity effect in older adults does not impair their capacity to feel negative emotions when seeing others' suffering. This underlines the importance of separately assessing negative and positive emotions, as done here and highlighted in previous research[49]

Finally, we found higher empathy correlated with increased negative affect during HE videos and with increased positive affect during LE videos, for both older and younger adults (Fig. 2c). However, positive emotions were reduced with higher empathy during HE videos only in older adults, suggesting that empathic effects on positive emotions in older people depend on context: the higher the empathy, the higher the positive emotions when facing social scenes without overt emotional content, but the lower the positive emotions when facing social scenes of others' distress. These data offer a perspective on how empathy may impact the 'positivity effect' usually observed in older adults.

Neural markers of negative social emotions and empathy

Negative socio-affective videos engaged brain regions overlapping with networks previously associated with social cognition and emotion[46,50]. These encompassed aMCC and AI, both implicated in empathy for pain[28,39], saliency detection[51,52] and negative affect[53], as well as TPJ and dMPFC, implicated in cognitive aspects of empathy and theory of mind[28,40]. In addition, in younger adults in experiment 1 and the larger sample of older adults in experiment 2, negative videos also activated the ventral striatum, an area associated with positive affect and reward[54] and recruited during compassion for other's suffering[45,46].

Remarkably, despite its prominent role in emotional processing, there was no significant activation in the amygdala during the HE > LE videos in either group. This null result might reflect a broader role in encoding social or self-relevant information rather than just negative valence[55], with the amygdala already activating to the content of LE videos and therefore showing similar increases during both video conditions in experiment 2 (Fig. 4h and Supplementary Fig. 2).

https://doi.org/10.1038/s43587-022-00341-6

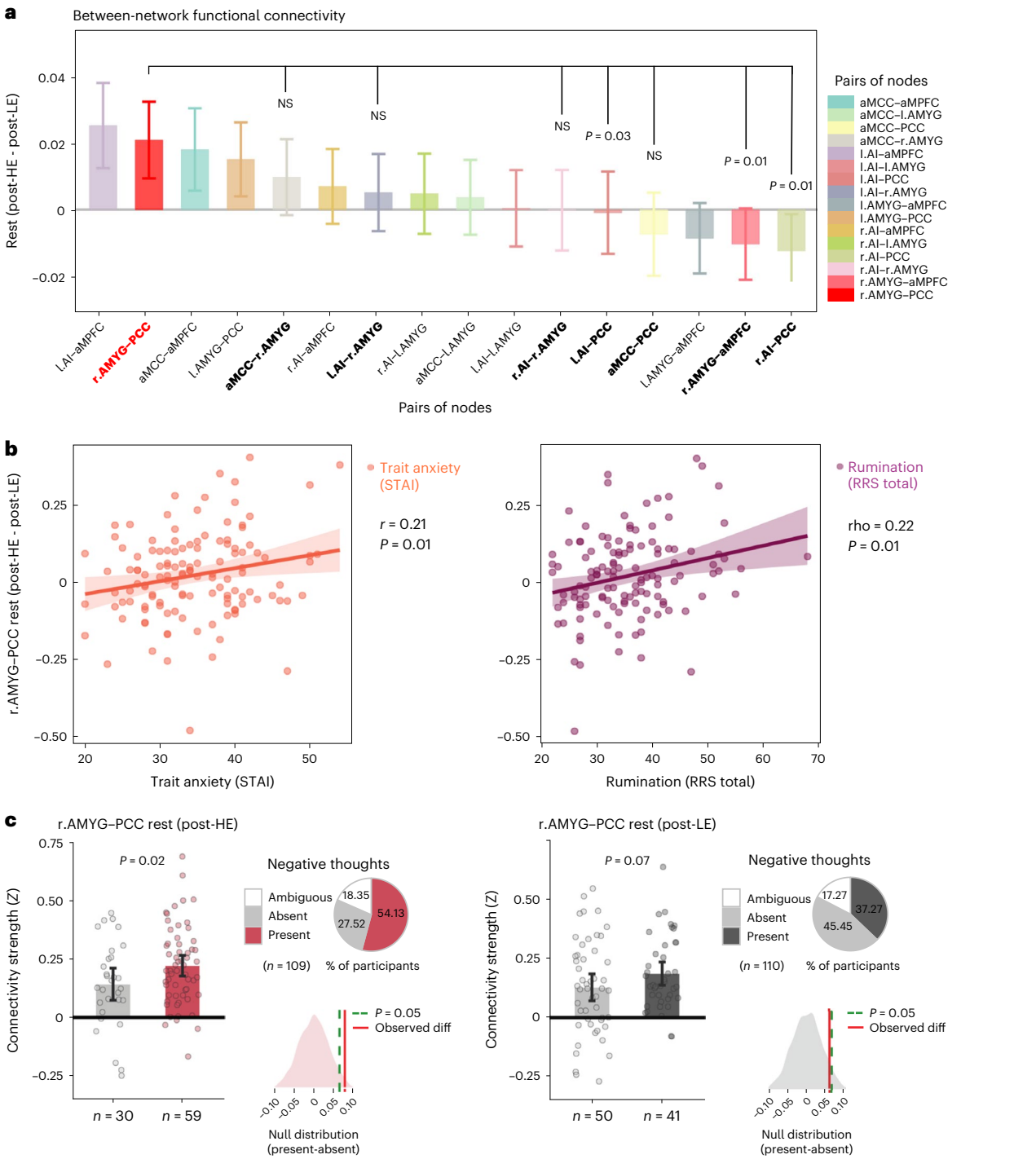

Fig. 6 | Between-network functional connectivity during rest periods after HE > LE videos. a, Pairs of nodes were ordered from left to right according to connectivity strength. The r.AMYG–PCC pair (red) was significantly more connected than other pairs involving either the PCC or the right amygdala (in bold). Significant comparisons from *t*-tests (one-tailed) are marked with corresponding *P* values; NS, not significant. **b**, Pearson (*r*) and Spearman (rho) correlations show that higher r.AMYG–PCC connectivity during rest periods after HE > LE videos was positively related to trait anxiety (STAI-trait) and rumination (RRS total). The shaded area represents the 95% confidence interval bands. **c**, Comparison of r.AMYG–PCC connectivity between the group who verbally reported negative content during thought probes (present) versus the group who did not (absent), for both HE and LE conditions. After HE videos, 59 (54%) participants reported negative content, 30 (28%) did not report negative content and 20 (18%) were ambiguous. After LE videos, only 41 (37%) reported negative content, 50 (45)% reported no negative thoughts and 19 (17%) were ambiguous. The mean r.AMYG–PCC connectivity difference was then compared between the two groups with versus without negative thoughts (observed difference = 0.08), relative to a null distribution built by permuting the labels 5,000 times. Participants reporting negative content in their thoughts (54%) versus those who did not (28%) showed higher r.AMYG–PCC connectivity in the HE condition ($P = 0.02$, one-tailed), but no difference in the LE condition (observed difference = 0.06; $P = 0.07$, one-tailed). Data for **a** and **c** depict mean values and error bars represent 95% confidence intervals. $N = 127$ older adults from experiment 2. Red indicates the HE condition; gray indicates the LE condition. r.AMYG–PCC indicates connectivity between the right amygdala and the PCC. Percentages in the text are rounded. Data are from experiment 2.

More critically, age affected brain responses to emotional scenes. Older adults activated less regions typically related to empathy (AI and PAG) and more those related to social cognition and emotion regulation (dMPFC, PCC and IFG). This accords with previous studies that examined age effects on empathy for pain[35,36] and empathy for negative and positive emotions[56]. Lower activity in affect-related regions, along with higher activity in cognition-related frontal regions might reflect better emotion regulation, possibly mediating the positivity effect of older people[1]. Increased activity in frontal regions may also reflect compensatory brain mechanisms acting to overcome cognitive deterioration in older adults[57]. In the current paradigm, these neural responses were not modulated by individual positive or negative affect scores, neither during videos nor during rest. Further research is needed to identify precise cognitive factors influencing emotional activation patterns in older adults, an issue beyond the purpose of the present study.

In sum, we find brain regions mediating empathy and Theory of Mind exhibit globally normal responses to negative social situations in healthy older adults. We also find positive affective biases in aging, seen in both behavioral and neural responses, indicating preserved socio-affective functions and empathy skills.

Emotional inertia after exposure to others' suffering

Beyond transient responses to negative stimuli, regulating the impact of emotions over time is crucial to cope with stressful events[58]. Emotional inertia denotes a persistence of emotional states reflecting inefficient recovery and greater risk for psychological maladjustment[12], but underlying neural substrates remain largely unexplored, especially in old populations. To uncover its neural underpinnings, we probed for emotional carryover effects in brain activity and assessed age-related differences. Across our two experiments, we observed selective increases during rest periods after HE (versus LE) videos. These comprised midline areas (ACC/MPFC and precuneus/PCC), involving core parts of the DMN typically active at rest[59], together with increases in amygdala and insula, critically implicated in emotional processing[29]. Importantly, these effects occurred only in older adults, suggesting an important modulation of emotion regulation mechanisms during aging. The DMN mediates self-related internally oriented processes, including memory, interoception and value-based decision-making[26]. Previous studies reported divergent findings on DMN reactivity to emotion, including decreases[17,18] or increases[19,25], similar to our results. Interestingly, the duration of DMN activation to negative stimuli correlates with subjective emotional intensity, better than response magnitude[19]. Here (experiment 2), we found that two midline nodes of DMN (precuneus/PCC and dMPFC) not only activated during the HE (versus LE) videos, but also continued their activity during subsequent rest (post-HE > post-LE), providing direct evidence for 'emotional inertia' in the aging brain. These findings resonate with previous work showing that older, but not younger, adults fail to deactivate DMN regions during cognitive tasks[33,34]. To our knowledge, these data reveal for the first time that increased DMN activation in older adults may persist over time after exposure to negative socio-emotional contexts.

Sustained changes were also observed in limbic regions in experiment 2. The AI showed increased activity during both (HE > LE) videos and (post-HE > post-LE) rest periods, although voxel-wise patterns did not fully overlap: videos produced a more dorsal engagement during videos responses, while the more ventral AI was active after emotional events. Given findings in younger adults[60] that dorsal AI may be recruited during adaptive behavior mechanisms, while ventral AI is recruited during internal homeostatic regulation, our result may reflect a shift from controlled/explicit adaptation to more spontaneous/implicit homeostatic regulation. On the other hand, the amygdala did not differentially respond during HE videos, but showed a lower return to baseline levels during post-HE (versus post-LE) rest. Accordingly, prolonged amygdala activity after negative images correlates with trait neuroticism[61], and enhanced amygdala response after negative emotion elicitation is amplified in high-anxiety individuals[15].

Altogether, our data highlight the temporal dynamics of brain responses to emotion and its relevance for individual affective styles and psychopathology[17,19,22].

Brain connectivity patterns related to emotional inertia

Our functional connectivity analysis revealed that post-emotional carryover implicated different circuits, linking core parts of the DMN (PCC and MPFC) with limbic regions (amygdala and AI). These connections were selectively enhanced in post-HE versus post-LE rest, exclusively in older adults, and across both experiments (Fig. 5). Further, PCC–amygdala connectivity was not only stronger for post-HE than post-LE conditions, but also selectively stronger than other between-network connectivity patterns involving either the PCC or the amygdala (Fig. 6a). Interestingly, the strength of PCC–amygdala connectivity predicted individual anxiety and rumination in older adults (experiment 2). Moreover, explicit verbal reports revealed more frequent negative thought contents during rest periods following HE videos, and participants with more frequent negative thoughts also had higher PCC–amygdala connectivity than those who reported no negative thoughts. Such a relationship between negative thoughts and PCC–amygdala connectivity was significantly weaker during post-LE rest. These findings suggest that increased functional connectivity between PCC and amygdala may support the persistence of negative contents in spontaneous thoughts.

PCC is involved in internally directed cognition, rumination and memory[26,62] especially when people retrieve affective autobiographical information[63]. As the amygdala also plays a central role in affective memory[27,55,64], we speculate that PCC–amygdala communication may contribute to emotional inertia and recovery from negative social situations, possibly through associations with personal affective memories, and especially in older adults with higher levels of anxiety and rumination. These data unveil age-related effects on neural processes associated with rumination and repetitive negative thinking, mental states associated not only with maladaptive emotion regulation but also with increased risk of cognitive decline and Alzheimer's disease[9,10]. As neurodegenerative anomalies in PCC and medial brain regions are common in Alzheimer's disease[65], changes in PCC connectivity might constitute a possible neural marker for deficient affective resilience, which is in turn associated with higher risk for dementia.

In parallel, increased functional connectivity was also observed between AI and aMPFC in post-HE versus post-LE rest in older adults from experiment 2. These changes showed no correlation with anxiety or rumination but only a weak positive correlation with the empathic concern IRI subscale (Supplementary Fig. 4). This may reflect a more general role of AI in emotional awareness[66] and empathy[28], and of aMPFC in the representation of affective states in both the self and others[47,67]. These results extend prior work by showing that connectivity between these two regions not only is modulated during the appraisal of socio-emotional stimuli but also persists beyond emotional events.

Limitations and future directions

Our study is not without limitations. First, participants watched videos passively, and subsequent carryover effects on brain activity and connectivity could reflect a lack of spontaneous implicit emotion regulation. Future studies should examine whether instructing participants with explicit emotion regulation strategies would change emotional inertia. Second, fMRI engendered technical constraints and affective ratings of videos were obtained only outside the scanner. Although this may bias the ratings, we deliberately made this choice to: (1) avoid top-down cognitive influences during scanning, which may confound neural activity during emotional perception;[68] and (2) maximize older adults' comfort by reducing the time spent inside the scanner. Third, parts of basal forebrain voxels were excluded from analyses in experiment 2

due to magnetic field inhomogeneities (Supplementary Fig. 5), as frequently induced in brain regions near air-filled cavities[69]. This prevented us from reliably studying regions such as the orbitofrontal cortex, despite their role in positive emotions and reward[45,54].

Conclusion

We show that empathy for suffering and affective resilience can reliably be investigated in older adults using the SoVT–rest, a paradigm with very low cognitive load and high ecological validity. Our results reveal neural and behavioral markers of the positivity bias in older adults and unveil sustained carryover effects (or emotional inertia) in corticolimbic brain circuits in healthy older adults. PCC–amygdala functional connectivity at rest was selectively increased following negative events, and such an increase was related to anxiety, rumination and negative thought content. This resting connectivity pattern constitutes a plausible neural substrate for emotional inertia. These findings provide an important cornerstone for better understanding empathy and mechanisms underlying affective resilience in the aging brain, and thus contribute to identifying potential risk markers for neurodegenerative diseases associated with poor social stress coping.

Methods

Participants

For experiment 1, a total of 58 healthy participants including 30 younger adults (aged between 19 and 30 years), and 28 older adults (aged between 65 and 78 years) with corrected-to-normal vision and no history of neurological, psychiatric disorder or alexithymia took part. Thirty individuals were expected to participate in each group; however, new research guidelines during the coronavirus disease 2019 pandemic prevented us from continuing with scanning. Recruitment was performed through social media and advertisement in various locations within the University of Geneva. Three participants were excluded due to a priori exclusion criteria, including artifacts in brain images and/or extreme head motion during scanning. The final sample for experiment 1 included 29 young participants (mean age, 24 years; 14 females) and 26 older participants (mean age, 68.7 years; 13 females), resulting in a total of $N = 55$ participants (see Table 1 for detailed participant characteristics). All participants provided written informed consent. This study was approved by the local Swiss ethics committee (Commission Cantonale d'Ethique de la Recherche CCRE, Geneva) under project number 2018–01980.

For experiment 2, a total of 137 healthy older adults participated, community-dwelling, with corrected-to-normal vision and no history of neurological or psychiatric disorders, aged between 65 and 83 years. This session was part of the baseline visit of the Age-Well randomized controlled trial (RCT) within the Medit-Ageing Project[70], conducted in Caen (France). Detailed inclusion criteria of the Age-Well RCT are provided in Supplementary Table 1. Participants were recruited via advertising in media outlets, social media and flyers distributed at relevant local events and locations. Two participants were excluded for eligibility criteria and intervention allocation issues[71]. A total of 8 participants were excluded from the final data analysis due to a priori exclusion criteria, including abnormal brain morphology ($n = 3$), extreme head motion ($n = 3$) and presence of artifacts in brain images ($n = 2$). The final sample for this study included 127 participants (mean age, 68.8 years, s.d. 3.63 years; 79 females; see Table 1 for other characteristics). All participants provided written informed consent before participation. The Age-Well RCT was approved by the ethics committee (Comité de Protection des Personnes Nord-Ouest III, Caen, France; trial registration number: EudraCT, 2016-002441-36; IDRCB, 2016-A01767-44; ClinicalTrials.gov identifier: NCT02977819).

Questionnaires

To account for interindividual differences in psycho-emotional profile, all participants from both experiments answered several questionnaires assessing psycho-affective traits and cognitive functions, including empathy (IRI[72]), depression (GDS[73] for older adults and BDI[74] for younger adults), anxiety (State-Trait Anxiety Inventory, STAI[75]), emotion regulation capacities (ERQ[76]) and rumination levels (RRS[77]). A summary of these questionnaires is provided in Table 1 and Fig. 1. All scores were in the normative range. For a full list of tasks and measures in the Age-Well trial (experiment 2), please refer to Poisnel and colleagues[70].

Socio-affective video task–rest

The emotion-elicitation task used in both experiments was adapted from the previously validated SoVT[43,45]. The SoVT aims to assess social emotions (for example, empathy) in response to short silent videos (10–18 s). During this task, participants watch 12 HE and 12 LE video clips grouped in blocks of three (see instructions in Supplementary Table 2). HE videos depict people suffering (for example, due to injuries or natural disasters), while LE videos depict people during everyday activities (for example, walking or talking). In this study, each block was followed by a resting-state period of 90 s (see instructions in Extended Data Fig. 1 and Supplementary Table 2) to assess the carryover effects of emotion elicitation on subsequent resting-state brain activity (similar to Eryilmaz and colleagues[17]). This combination of both paradigms (task and rest) was specifically designed to test for emotional inertia and its relation to empathy. The combined task (SoVT–rest) is illustrated in Extended Data Fig. 1.

Overall, three sets (V1, V2 and V3) of 24 videos each were created and randomized across participants. In experiment 1, the video sets V1, V2 and V3 were seen by $n = 21$, 18 and 16 participants, respectively. In experiment 2, these were seen by $n = 42$, 40 and 45 participants, respectively. In both experiments, these videos were presented in two separate runs, always followed by a rest period. In experiment 2, each run was followed by a thought probe to assess current mental content during the last rest period (after LE videos in one run and after HE videos in the other run). The order in which runs were presented was randomized so that half of the participants started the experiment with a HE block and the other half with an LE block. No thought probe was given in experiment 1 (as it primarily aims at determining age-related brain activity patterns at rest). Brief instructions (in French) were presented before each period within each block. These indicated 'The task is about to start' before the first period of videos, or 'The next videos are going to start' before those in the following periods; while the display 'Rest: wait for the next videos' appeared before each rest period (Extended Data Fig. 1a,b). The total duration of the SoVT–rest fMRI paradigm was approximately 21 min, consisting of 9.5 min for each run, plus 1 min on average for the thought probes.

After the fMRI session, participants watched all video clips again on a computer outside the scanner and provided ratings on their subjective experience of empathy ('To what degree did you feel the emotions of the characters?') as well as their subjective positive affect ('Indicate the intensity of your positive emotions') and negative affect state ('Indicate the intensity of your negative emotions'; translated from French), for each of the 24 videos. Each scale offered 21 possible responses ranging from 0 ('not at all') to 10 ('extremely') with increments of 0.5. The order of questions was always the same: empathy, positive affect and negative affect. We chose to obtain ratings after fMRI not only to minimize the time older adults spent in the scanner, but also to avoid potential cognitive effects during scanning that may confound neural activity during emotional perception and spontaneous rest recovery periods[68,78]. The total time for post-scanning ratings was, on average, 10 min. Onset times and response times for both neuroimaging and behavioral tasks were collected via the Cogent toolbox (developed by Cogent 2000 and Cogent Graphics) implemented in MATLAB 2012 (MathWorks).

Acquisition and preprocessing of magnetic resonance imaging data

Experiment 1. MRI scans were acquired at the Brain and Behavior Laboratory of the University of Geneva, using a 3T whole-body MRI scanner (Trio TIM, Siemens) with the 32-channel head coil. A high-resolution

T1-weighted anatomical volume was first acquired using a magnetization-prepared rapid acquisition gradient echo (MPRAGE) sequence (repetition time, 1,900 ms; echo time, 2.27 ms; flip angle, 9°; slice thickness, 1 mm; field of view, 256 × 256 mm^2; in-plane resolution, 1 × 1 mm^2). Blood oxygen level-dependent (BOLD) images were acquired with a susceptibility-weighted EPI sequence (TR/TE, 2,000/30 ms; flip angle, 85°; voxel size, 3 × 3 mm; 35 slices, 3-mm-slice thickness, 20% slice gap; direction of acquisition, descending). Quality control and preprocessing were conducted using Statistical Parametric Mapping software (SPM12; Wellcome Trust Centre for Neuroimaging) on MATLAB 2017 (MathWorks). Before preprocessing, we manually centered all images to the AC-PC axis, aligned the functional and anatomical MRI images, and then realigned all images to the SPM anatomical template. Preprocessing included the following steps: (1) EPI data were realigned to the first volume and spatially smoothed with an 8-mm FWHM Gaussian kernel; (2) preprocessed fMRI data were denoised for secondary head motion and cerebrospinal fluid-related artifacts using automatic noise selection as implemented in ICA-AROMA, a method for distinguishing noise-related components based on ICA decomposition[79]. Additionally, components with high spatial overlap with white-matter regions were also removed by means of a linear regression using the fsl_regfilt function of FSL 6.0 (FMRIB's Software Library; https://fsl.fmrib.ox.ac.uk/fsl/fslwiki/); (3) denoised EPI data were co-registered to the anatomical T1 volume; (4) the anatomical T1 volume was segmented and the extracted parameters were used to (5) normalize all EPI volumes into the Montreal Neurological Institute space. This procedure was performed using FSL and SPM12.

Experiment 2. MRI scans were acquired at the GIP Cyceron using a Philips Achieva 3T scanner with a 32-channel head coil. Participants were provided with earplugs to protect hearing, and their heads were stabilized with foam pads to minimize head motion. A high-resolution T1-weighted anatomical volume was first acquired using a three-dimensional fast field echo sequence (3D-T1-FFE sagittal; repetition time, 7.1 ms; echo time, 3.3 ms; flip angle, 6°; 180 slices with no gap; slice thickness, 1 mm; field of view, 256 × 256 mm^2; in-plane resolution, 1 × 1 mm^2). BOLD images were acquired during the SoVT–rest task with a T2*-weighted asymmetric spin-echo echo-planar sequence (each run ~10.5 min; TR, 2,000 ms; TE, 30 ms; flip angle, 85°; FOV, 240 × 240 mm^2; matrix size, 80 × 68 × 33; voxel size, 3 × 3 × 3 mm^3; slice gap, 0.6 mm) in the axial plane parallel to the anteroposterior commissure. During each functional run, about 310 contiguous axial images were acquired and the first two images were discarded because of saturation effects. Additionally, to improve the preprocessing and enhance the quality of the BOLD images[80], T2 and T2* structural volumes were collected. Each functional and anatomical image was visually inspected to discard susceptibility artifacts and anatomical abnormalities.

Quality control and preprocessing were conducted using statistical parametric mapping software (SPM12; Wellcome Trust Centre for Neuroimaging) on MATLAB 2017 (MathWorks). Before preprocessing, we manually centered the images to the AC-PC axis, realigned the functional and anatomical MRI images and then realigned all images to the last version of the SPM anatomical template. The preprocessing procedure was done with SPM12 and followed a methodology designed to reduce geometric distortion effects induced by the magnetic field, described by Villain and colleagues[80]. This procedure included the following steps: (1) realignment of the EPI volumes to the first volume and creation of the mean EPI volume; (2) co-registration of the mean EPI volume and anatomical T1, T2 and T2* volumes; (3) warping of the mean EPI volume to match the anatomical T2* volume, and application of the deformation parameters to all the EPI volumes; (4) segmentation of the anatomical T1 volume; (5) normalization of all the EPIs, T1 and T2* volumes into the Montreal Neurological Institute space using the parameters obtained during the T1 segmentation; (6) 8-mm FWHM smoothing of the EPI volumes.

For each individual, frame-wise displacement (FD)[81] was calculated. FD values greater than 0.5 mm were flagged to be temporally censored or 'scrubbed' during the first-level analysis (see description below). The average of FD volumes censored was 6.8 (s.d. 8.3, minimum of 1, maximum of 38) for both runs for a total of $n = 65$ participants. Three participants were excluded from further analysis because >10% of volumes showed FD > 0.5 mm within one run.

General linear model analysis

For both experiments, the MRI SoVT–rest data were analyzed using GLMs in SPM12 (implemented in MATLAB 2017). This comprised standard first-level analyses at the subject level, followed by random-effect (second-level) analyses to assess the effects of interest at the group level. For the first-level analysis, a design matrix consisting of two separate sessions was constructed for each participant. Experimental event regressors in each session included the fixation cross (10 s), instructions (8 s in experiment 1, 4 s in experiment 2), the three videos (~15 s each) modeled separately, and the rest periods following each block (90 s). Each rest period was divided into three equal parts (30 s time bins) to model different time intervals during which brain activity may gradually change after the end of the HE and LE video blocks (similar to Eryilmaz and colleagues[17]).

The different regressors were then convolved with a hemodynamic response function according to a block design for univariate regression analysis. To account for motion confounds, the six realignment parameters were added to the matrices, and low-frequency drifts were removed via a high-pass filter (cutoff frequency at 1/256 Hz). The final first-level matrix consisted of 2 sessions of 21 regressors each (1 fixation cross + 1 instruction for videos + 1 instructions for rest + 3 HE videos + 3 post-HE rest + 3 LE videos + 3 post-LE rest + 6 motion parameters). Additionally, we addressed the influence of remaining motion on BOLD data by performing data censoring as described by Power and colleagues[81]. Specifically, during the estimation of beta coefficients for each regressor of interest, volumes with FD > 0.5 mm were flagged in the design matrices and ignored during the estimation of the first levels.

For the second-level analyses, we used flexible factorial designs where the estimated parameters from first-level contrasts of interest were entered separately for each participant. The second-level design matrix was generated with SPM12 and included 12 regressors of interest (3 HE videos + 3 post-HE rest + 3 LE videos + 3 post-LE rest). This step allowed us to investigate the effect of each experimental condition on brain activity, including the main condition effects (video and rest), the specific emotional effects (HE and LE) during either the video or the subsequent rest periods as well as the age effect on the different conditions (young versus old; experiment 1).

Functional connectivity during rest periods

For both experiments, we conducted functional connectivity analyses between the most important brain ROIs associated with the empathy network and with the DMN. In addition, we also included the bilateral amygdalae among regions used for this analysis because previous studies assessing carryover effects in the brain have related sustained amygdala activity to anxiety traits[15] and emotional reactivity[61]. For nodes of the DMN, we chose the PCC and the aMPFC, following Andrews-Hanna and colleagues[59]. Based on the results of a meta-analysis by Fan and colleagues[39], the bilateral AI and aMCC were used as ROIs in the empathy network. Time series were extracted from 6-mm-radius spheres around the peak of each of these ROIs. The amygdala was defined anatomically using the current SPM anatomical template provided by Neuromorphometrics (http://neuromorphometrics.com/).

Functional connectivity analyses were performed using MATLAB 2017 and R studio (version 3.6.1). For each participant, time courses of activity (from each voxel of the brain) were high-pass filtered at 256 Hz, de-trended and standardized (z-score) before extracting specific time courses from the defined ROIs. In addition, white matter, cerebrospinal

fluid signals, and realignment parameters were included as nuisance regressors in experiment 2. For each participant, time series from the instructions and videos periods were removed, and the remaining time series corresponding to the rest periods were concatenated. This procedure was previously proposed by Fair and colleagues[82] and proved to be qualitatively and quantitatively very similar to continuous resting-state data. Additionally, to correct extreme head motion without affecting the autocorrelation of the time series, image volumes flagged with FD > 0.5 mm were removed and replaced by interpolation (every flagged volume X was replaced by the estimated mean of the $X-1$ and $X+1$ volumes). The final concatenated time series resulted in 184 frames (~386 s) of resting-state data for each participant. We then correlated the time courses between the different ROIs using Pearson correlations, and the resulting coefficients were subjected to Fisher's r-to-z transformation to improve normality in the data. Individual z-score maps (correlation matrices) were created for each participant (Extended Data Fig. 2a,b,c).

Thought probes

For each participant in experiment 2, two thought probes were recorded after the last rest period of each run and subsequently analyzed to test for differences in spontaneous mind wandering after emotional videos. Participants freely described their thoughts, and these narratives were digitally recorded and transcribed for analyses by two independent raters (Supplementary Table 4). For each probe (post-HE rest and post-LE rest), the two raters attributed the presence (present) or the absence (absent) of specific thought contents according to a diverse set of predefined categories (Supplementary Table 4). These categories were selected according to a priori relevant affective or cognitive dimensions, and included the following: negative and positive emotions, directed attention to oneself and to others, emotion regulation (voluntary control of emotions), negative and positive social emotions, rumination and temporality (present or past/future). Categories with low variability (that is, the same thought content reported by more than 85% of participants) were not included in further analyses because this prevented reliable regression analysis (Supplementary Table 4). The final dimensions included negative and positive emotions, directed attention to oneself and to others, and positive social emotions. This final analysis of thought probes comprised data from 109 participants for rest periods after HE videos and 110 participants for the rest periods after LE videos. This was due to (1) missing thought probes for 9 participants and (2) exclusion of reports not referring directly to thoughts or feelings in the rest period (but rather to factual details in the videos) for both runs ($n = 5$), following LE rest ($n = 3$) or following HE rest ($n = 4$). Inter-rater agreement on the final dimensions ranged from 0.28 to 0.66 (Cohen's kappa index; Supplementary Table 4 for details). The statistical analyses were performed with R studio (version 3.6.1) and the corresponding graphs were created with ggplot2 (version 3.2.1).

Statistics and reproducibility

Statistical analyses of behavioral data. We performed a repeated-measures multivariate analysis of variance (with Pillai's trace statistics) with the within-subject factor 'video type' (HE and LE), the between-subject factor 'video set' (V1, V2 and V3) and three dependent variables: ratings of empathy, positive affect and negative affect. This was followed up by pairwise t-tests. We also computed Spearman's rank correlations between these different scores. Additionally, we performed correlation analyses between ratings of empathy, positive affect and negative affect of videos and age (as a continuous variable), using non-parametric Spearman's rank correlations because some of these variables were not normally distributed. All statistical analyses are reported with a significance level of $P < 0.05$, and when necessary, P values were corrected for multiple comparisons using the FDR method[83]. Normality in the data was tested, and non-parametrical tests (for example, Spearman's rank correlations) were performed when estimated necessary.

Statistical analyses of brain activity. In both experiments, we conducted t-tests contrasts to compare the conditions of interest (videos versus rest periods and vice versa) and the specific emotional effects (videos, HE versus LE; rest, HE versus LE). In experiment 1, we additionally tested for age differences in these effects (OAs versus YAs (videos, HE versus LE); OAs versus YAs (rest, HE versus LE)). In experiment 1, results are reported at uncorrected $P < 0.001$, $k > 20$ because this dataset concerned a smaller sample size and aimed at defining a comprehensive set of brain regions with emotion-related modulations in either videos or rest period in either age group. These regions could then be further probed with higher reliability and related to relevant individual characteristics in the larger dataset of experiment 2. Moreover, a more permissive combination of voxel-based and cluster-based thresholds has been shown to be adequate and reliable for experiments assessing cognitive and affective processes with unprecise onsets[84], as in our task–rest paradigm. In addition, we had strong predictions concerning relevant regions (for example, DMN) based on previous works[17,24,43]. Finally, clusters surviving whole-brain family-wise error correction at $P < 0.05$ at the cluster level (FWEc) in experiment 1 are indicated in figures and tables (Supplementary Table 3a). In experiment 2, all comparisons are reported with a whole-brain FWE correction at $P < 0.05$, at the voxel level (Supplementary Table 3b).

Statistical analyses of brain functional connectivity. To test for significant differences between the two correlation matrices (post-HE rest and post-LE rest), we used a non-parametric permutation test[85]. For each pair of nodes, the permutation test compared the true correlation difference (for example, HE − LE) to a null distribution built by randomly flipping the sign of the correlation coefficients and computing the difference many times ($n = 5{,}000$; Extended Data Fig. 2d). More precisely, for each pair of nodes (for example, HE − LE for ROI 1 and ROI 3), a vector of values of n = number of participants was obtained and a one-sample t-test was computed to obtain the real t value (t_{real}). Then, the signs of the elements in the vector were randomly flipped ($n = 5{,}000$) and the model was fitted repeatedly once for every flipping. For each fit, a new realization of the t-statistic was computed to construct an empirical distribution of t under the null hypothesis ($t_{permuted}$). From this null distribution, a P value was computed by assessing the probability of the t_{real} to be higher than 95% of the values on the empirical $t_{permuted}$ distribution[85]. Finally, the obtained P values were converted into an equivalent z-score and significant changes (marked by an asterisk in matrices) were retained for $z > 1.64$ (equivalent to $P < 0.05$, one-tailed, given observed increases without decreases in GLM analysis, uncorrected).

The final sample for experiment 1 included $N = 55$ participants. Three participants were excluded due to a priori exclusion criteria, including artifacts in brain images and/or extreme head motion during scanning. No statistical methods were used to predetermine sample sizes but our sample sizes are similar to those reported in previous publications[17,35]. The final sample for experiment 2 included $N = 127$ participants. Two participants were excluded for eligibility criteria and intervention allocation issues[71]. Eight participants were excluded from the final data analysis due to a priori exclusion criteria: abnormal brain morphology ($n = 3$), extreme head motion ($n = 3$) and presence of artifacts in brain images ($n = 2$). For the primary outcome of the Age-well RCT, an effect size of 0.75 per comparison was targeted, with 80% power and a two-sided type I error of 1.25% (Bonferroni correction for test multiplicity), resulting in a total of 126 participants needing to be included. The final number of participants in the Age-Well RCT ($n = 137$) was higher than the required minimum of 126 participants[70,71]. Sensitivity analyses then indicated that the final sample included in experiment 2 ($n = 127$) was reliable and sensitive enough to detect small- to medium-sized effects at a voxel level ($\alpha = 0.001$, effect size of $dz = 0.37$), given a power of $1 - \beta = 0.8$ (ref. 86). For both experiments, the video sets (V1, V2 and V3) and whether participants started the experiment

with HE or LE videos first were randomly attributed to participants in an Excel table. While investigators were blinded to the training arm that participants were randomized to in the Age-Well trial, no blinding was performed for the SoVT–rest task at baseline (experiment 2). The statistical analyses were performed with R studio (version 3.6.1) and MATLAB 2017 (MathWorks), and the corresponding graphs were created with ggplot2 (version 3.2.1).

Reporting summary

Further information on research design is available in the Nature Portfolio Reporting Summary linked to this article.

Data availability

The data underlying this report are available on request following a formal data sharing agreement and approval by the consortium and executive committee (https://silversantestudy.eu/2020/09/25/data-sharing/). The material can be mobilized, under the conditions and modalities defined in the Medit-Ageing Charter, by any research team belonging to an Academic for carrying out a scientific research project relating to the scientific theme of mental health and well-being in older people. The material may also be mobilized by nonacademic third parties, under conditions, in particular financial, which will be established by separate agreement between Inserm and by the said third party. Data sharing policies described in the Medit-Ageing Charter are in compliance with our ethics approval and guidelines from our funding body.

Code availability

The code used to produce the results reported herein can be made available upon appropriate request.

References

1. Mather, M. The affective neuroscience of aging. *Annu. Rev. Psychol.* https://doi.org/10.1146/annurev-psych-122414-033540 (2015).
2. Reiter, A. M. F., Kanske, P., Eppinger, B. & Li, S.-C. The aging of the social mind—differential effects on components of social understanding. *Sci Rep.* **7**, 11046 (2017).
3. Urry, H. L. & Gross, J. J. Emotion regulation in older age. *Curr. Dir. Psychol. Sci.* **19**, 352–357 (2010).
4. Mather, M. & Carstensen, L. L. Aging and motivated cognition: the positivity effect in attention and memory. *Trends Cogn. Sci.* **9**, 496–502 (2005).
5. Aldao, A., Nolen-Hoeksema, S. & Schweizer, S. Emotion-regulation strategies across psychopathology: a meta-analytic review. *Clin. Psychol. Rev.* **30**, 217–237 (2010).
6. Hamilton, J. P., Farmer, M., Fogelman, P. & Gotlib, I. H. Depressive rumination, the default-mode network, and the dark matter of clinical neuroscience. *Biol. Psychiatry* **78**, 224–230 (2015).
7. Kraaij, V., Pruymboom, E. & Garnefski, N. Cognitive coping and depressive symptoms in the elderly: a longitudinal study. *Aging Ment. Health* **6**, 275–281 (2002).
8. Terracciano, A. et al. Personality and risk of Alzheimer's disease: new data and meta-analysis. *Alzheimers Dement.* **10**, 179–186 (2014).
9. Marchant, N. L. & Howard, R. J. Cognitive debt and Alzheimer's disease. *J. Alzheimers Dis.* **44**, 755–770 (2015).
10. Marchant, N. L. et al. Repetitive negative thinking is associated with amyloid, tau, and cognitive decline. *Alzheimers Dement.* https://doi.org/10.1002/alz.12116 (2020).
11. Jané-Llopis, E. & Gabilondo, A. Mental Health in Older People. Consensus paper. Luxembourg: European Communities (2008).
12. Kuppens, P., Allen, N. B. & Sheeber, L. B. Emotional inertia and psychological maladjustment. *Psychol. Sci.* **21**, 984–991 (2010).
13. Koval, P., Kuppens, P., Allen, N. B. & Sheeber, L. Getting stuck in depression: the roles of rumination and emotional inertia. *Cogn. Emot.* **26**, 1412–1427 (2012).
14. Van De Leemput, I. A. et al. Critical slowing down as early warning for the onset and termination of depression. *Proc. Natl Acad. Sci. USA* **111**, 87–92 (2014).
15. Pichon, S., Miendlarzewska, E. A., Eryilmaz, H. & Vuilleumier, P. Cumulative activation during positive and negative events and state anxiety predicts subsequent inertia of amygdala reactivity. *Soc. Cogn. Affect. Neurosci.* **10**, 180–190 (2015).
16. Lamke, J. P. et al. The impact of stimulus valence and emotion regulation on sustained brain activation: task–rest switching in emotion. *PLoS ONE* **9**, e93098 (2014).
17. Eryilmaz, H., Van De Ville, D., Schwartz, S. & Vuilleumier, P. Impact of transient emotions on functional connectivity during subsequent resting state: a wavelet correlation approach. *Neuroimage* **54**, 2481–2491 (2011).
18. Pitroda, S., Angstadt, M., McCloskey, M. S., Coccaro, E. F. & Phan, K. L. Emotional experience modulates brain activity during fixation periods between tasks. *Neurosci. Lett.* **443**, 72–76 (2008).
19. Waugh, C. E., Hamilton, J. P. & Gotlib, I. H. The neural temporal dynamics of the intensity of emotional experience. *Neuroimage* **49**, 1699–1707 (2010).
20. Veer, I. M. et al. Beyond acute social stress: increased functional connectivity between amygdala and cortical midline structures. *Neuroimage* **57**, 1534–1541 (2011).
21. Eryilmaz, H., Van De Ville, D., Schwartz, S. & Vuilleumier, P. Lasting impact of regret and gratification on resting brain activity and its relation to depressive traits. *J. Neurosci.* **34**, 7825–7835 (2014).
22. Waugh, C. E., Hamilton, J. P., Chen, M. C., Joormann, J. & Gotlib, I. H. Neural temporal dynamics of stress in comorbid major depressive disorder and social anxiety disorder. *Biol. Mood Anxiety Disord.* **2**, 11 (2012).
23. Northoff, G., Qin, P. & Nakao, T. Rest-stimulus interaction in the brain: a review. *Trends Neurosci.* **33**, 277–284 (2010).
24. Gaviria, J., Rey, G., Bolton, T., Van De Ville, D. & Vuilleumier, P. Dynamic functional brain networks underlying the temporal inertia of negative emotions. *Neuroimage* **240**, 118377 (2021).
25. Schneider, F. et al. The resting brain and our self: self-relatedness modulates resting state neural activity in cortical midline structures. *Neuroscience* **157**, 120–131 (2008).
26. Buckner, R. L., Andrews-Hanna, J. R. & Schacter, D. L. The brain's default network: anatomy, function, and relevance to disease. *Ann. N. Y. Acad. Sci.* **1124**, 1–38 (2008).
27. LeDoux, J. The emotional brain, fear, and the amygdala. *Cell. Mol. Neurobiol.* https://doi.org/10.1023/A:1025048802629 (2003).
28. Lamm, C., Decety, J. & Singer, T. Meta-analytic evidence for common and distinct neural networks associated with directly experienced pain and empathy for pain. *Neuroimage* **54**, 2492–2502 (2011).
29. Meaux, E. & Vuilleumier, P. Emotion Perception and Elicitation. In: *Brain Mapping: An Encyclopedic Reference* (ed Toga, A. W.) 79–90 (Academic Press, San Diego, CA, USA, 2015).
30. Kim, M. J. et al. The structural and functional connectivity of the amygdala: from normal emotion to pathological anxiety. *Behav. Brain Res.* **223**, 403–410 (2011).
31. Rey, G. et al. Resting-state functional connectivity of emotion regulation networks in euthymic and non-euthymic bipolar disorder patients. *Eur. Psychiatry* **34**, 56–63 (2016).
32. Carstensen, L. L., Mayr, U., Pasupathi, M. & Nesselroade, J. R. Emotional experience in everyday life across the adult lifespan. *J. Pers. Soc. Psychol.* **79**, 644–655 (2000).
33. Spreng, R. N. & Schacter, D. L. Default network modulation and large-scale network interactivity in healthy young and old adults. *Cereb. Cortex* **22**, 2610–2621 (2012).

34. Turner, G. R. & Spreng, R. N. Prefrontal engagement and reduced default network suppression co-occur and are dynamically coupled in older adults: the default-executive coupling hypothesis of aging. *J. Cogn. Neurosci.* **27**, 2462–2476 (2015).
35. Chen, Y. -C., Chen, C. -C., Decety, J. & Cheng, Y. Aging is associated with changes in the neural circuits underlying empathy. *Neurobiol. Aging* **35**, 827–836 (2014).
36. Tamm, S. et al. The effect of sleep restriction on empathy for pain: an fMRI study in younger and older adults. *Sci. Rep.* **7**, 12236 (2017).
37. Beadle, J. N. & De La Vega, C. E. Impact of aging on empathy: review of psychological and neural mechanisms. *Front. Psychiatry* **10**, 331 (2019).
38. Sze, J. A., Gyurak, A., Goodkind, M. S. & Levenson, R. W. Greater emotional empathy and prosocial behavior in late life. *Emotion* **12**, 1129–1140 (2012).
39. Fan, Y., Duncan, N. W., de Greck, M. & Northoff, G. Is there a core neural network in empathy? An fMRI-based quantitative meta-analysis. *Neurosci. Biobehav. Rev.* **35**, 903–911 (2011).
40. Schurz, M., Radua, J., Aichhorn, M., Richlan, F. & Perner, J. Fractionating theory of mind: a meta-analysis of functional brain imaging studies. *Neurosci. Biobehav. Rev.* **42**, 9–34 (2014).
41. Krueger, K. R. et al. Social engagement and cognitive function in old age. *Exp. Aging Res.* **35**, 45–60 (2009).
42. MacLeod, S., Musich, S., Hawkins, K., Alsgaard, K. & Wicker, E. R. The impact of resilience among older adults. *Geriatr. Nurs.* **37**, 266–272 (2016).
43. Klimecki, O. M., Leiberg, S., Lamm, C. & Singer, T. Functional neural plasticity and associated changes in positive affect after compassion training. *Cereb. Cortex* **23**, 1552–1561 (2013).
44. Wancata, J., Alexandrowicz, R., Marquart, B., Weiss, M. & Friedrich, F. The criterion validity of the Geriatric Depression Scale: a systematic review. *Acta Psychiatr. Scand.* **114**, 398–410 (2006).
45. Klimecki, O. M., Leiberg, S., Ricard, M. & Singer, T. Differential pattern of functional brain plasticity after compassion and empathy training. *Soc. Cogn. Affect. Neurosci.* **9**, 873–879 (2013).
46. Singer, T. & Klimecki, O. M. Empathy and compassion. *Curr. Biol.* **24**, R875–R878 (2014).
47. Corradi-Dell'Acqua, C., Hofstetter, C. & Vuilleumier, P. Cognitive and affective Theory of Mind share the same local patterns of activity in posterior temporal but not medial prefrontal cortex. *Soc. Cogn. Affect. Neurosci.* **9**, 1175–1184 (2014).
48. Klimecki, O. M. et al. The impact of meditation on healthy ageing—the current state of knowledge and a roadmap to future directions. *Curr. Opin. Psychol.* **28**, 223–228 (2019).
49. Cacioppo, J. T. & Berntson, G. G. Relationship between attitudes and evaluative space: a critical review, with emphasis on the separability of positive and negative substrates. *Psychol. Bull.* **115**, 401–423 (1994).
50. Preckel, K., Kanske, P. & Singer, T. On the interaction of social affect and cognition: empathy, compassion and theory of mind. *Curr. Opin. Behav. Sci.* **19**, 1–6 (2018).
51. Seeley, W. W. et al. Dissociable intrinsic connectivity networks for salience processing and executive control. *J. Neurosci.* **27**, 2349–2356 (2007).
52. Menon, V. & Uddin, L. Q. Saliency, switching, attention and control: a network model of insula function. *Brain Struct. Funct.* **214**, 655–667 (2010).
53. Knutson, B., Katovich, K. & Suri, G. Inferring affect from fMRI data. *Trends. Cogn. Sci.* **18**, 422–428 (2014).
54. Knutson, B., Fong, G. W., Adams, C. M., Varner, J. L. & Hommer, D. Dissociation of reward anticipation and outcome with event-related fMRI. *Neuroreport* **12**, 3683–3687 (2001).
55. Sander, D., Grafman, J. & Zalla, T. The human amygdala: an evolved system for relevance detection. *Rev. Neurosci.* **14**, 303–316 (2003).
56. Riva, F. et al. Age-related differences in the neural correlates of empathy for pleasant and unpleasant touch in a female sample. *Neurobiol. Aging* **65**, 7–17 (2018).
57. Davis, S. W., Dennis, N. A., Daselaar, S. M., Fleck, M. S. & Cabeza, R. Qué PASA? The posterior–anterior shift in aging. *Cereb. Cortex* **18**, 1201–1209 (2008).
58. Davidson, R. J. Affective style and affective disorders: perspectives from affective neuroscience. *Cogn. Emot.* **12**, 307–330 (1998).
59. Andrews-Hanna, J. R., Reidler, J. S., Sepulcre, J., Poulin, R. & Buckner, R. L. Functional-anatomic fractionation of the brain's default network. *Neuron* **65**, 550–562 (2010).
60. Lamm, C. & Singer, T. The role of anterior insular cortex in social emotions. *Brain Struct. Funct.* **214**, 579–591 (2010).
61. Schuyler, B. S. et al. Temporal dynamics of emotional responding: amygdala recovery predicts emotional traits. *Soc. Cogn. Affect. Neurosci.* **9**, 176–181 (2014).
62. Makovac, E., Fagioli, S., Rae, C. L., Critchley, H. D. & Ottaviani, C. Can't get it off my brain: meta-analysis of neuroimaging studies on perseverative cognition. *Psychiatry Res. Neuroimaging* **295**, 111020 (2020).
63. Addis, D. R., Wong, A. T. & Schacter, D. L. Remembering the past and imagining the future: common and distinct neural substrates during event construction and elaboration. *Neuropsychologia* **45**, 1363–1377 (2007).
64. Phelps, E. A. & LeDoux, J. E. Contributions of the amygdala to emotion processing: from animal models to human behavior. *Neuron* **48**, 175–187 (2005).
65. Jagust, W. Imaging the evolution and pathophysiology of Alzheimer disease. *Nat. Rev. Neurosci.* https://doi.org/10.1038/s41583-018-0067-3 (2018).
66. Critchley, H. D., Wiens, S., Rotshtein, P., Öhman, A. & Dolan, R. J. Neural systems supporting interoceptive awareness. *Nat. Neurosci.* **7**, 189–195 (2004).
67. Amodio, D. M. & Frith, C. D. Meeting of minds: the medial frontal cortex and social cognition. *Nat. Rev. Neurosci.* **7**, 268–277 (2006).
68. Grimm, S. et al. Segregated neural representation of distinct emotion dimensions in the prefrontal cortex—an fMRI study. *Neuroimage* **30**, 325–340 (2006).
69. Juchem, C., Nixon, T. W., McIntyre, S., Rothman, D. L. & De Graaf, R. A. Magnetic field homogenization of the human prefrontal cortex with a set of localized electrical coils. *Magn. Reson. Med.* **63**, 171–180 (2010).
70. Poisnel, G. et al. The Age-Well randomized controlled trial of the Medit-Ageing European project: effect of meditation or foreign language training on brain and mental health in older adults. *Alzheimers Dement.* **4**, 714–723 (2018).
71. Chételat, G. et al. Effect of an 18-month meditation training on regional brain volume and perfusion in older adults: The Age-Well Randomized Clinical Trial. *JAMA Neurol.* https://doi.org/10.1001/jamaneurol.2022.3185 (2022).
72. Davis, M. H. Measuring individual differences in empathy: Evidence for a multidimensional approach. *J. Pers. Soc. Psychol.* **44**, 113–126 (1983).
73. Sheikh, J. I. & Yesavage, J. A. Geriatric Depression Scale (GDS) recent evidence and development of a shorter version. *Clin. Gerontol.* https://doi.org/10.1300/J018v05n01_09 (1986).
74. Beck, A. T., Steer, R. A., Ball, R. & Ranieri, W. F. Comparison of Beck Depression Inventories-IA and-II in psychiatric outpatients. *J. Pers. Assess.* **67**, 588–597 (1996).

75. Spielberger, C. D., Gorsuch, R. L. & Lushene, R. *State–Trait Anxiety Inventory STAI (Form Y)*. Redwood City: Mind Garden. https://doi.org/10.1515/9783111677439-035 (1983).
76. Gross, J. J. & John, O. P. Individual differences in two emotion regulation processes: implications for affect, relationships, and well-being. *J. Pers. Soc. Psychol.* **85**, 348–362 (2003).
77. Treynore, G. & Nolen-Hoeksema, S. Ruminative Responses Scale. *Cogn. Ther. Res.* https://doi.org/10.1017/CBO9781107415324.004 (2003).
78. Taylor, W. D. et al. Smaller orbital frontal cortex volumes associated with functional disability in depressed elders. *Biol. Psychiatry* **53**, 144–149 (2003).
79. Pruim, R. H. R. et al. ICA-AROMA: a robust ICA-based strategy for removing motion artifacts from fMRI data. *Neuroimage* **112**, 267–277 (2015).
80. Villain, N. et al. A simple way to improve anatomical mapping of functional brain imaging. *J. Neuroimaging* **20**, 324–333 (2010).
81. Power, J. D., Barnes, K. A., Snyder, A. Z., Schlaggar, B. L. & Petersen, S. E. Spurious but systematic correlations in functional connectivity MRI networks arise from subject motion. *Neuroimage* **59**, 2142–2154 (2012).
82. Fair, D. A. et al. A method for using blocked and event-related fMRI data to study 'resting state' functional connectivity. *Neuroimage* **35**, 396–405 (2007).
83. Benjamini, Y. & Hochberg, Y. Controlling the false discovery rate: a practical and powerful approach to multiple testing. *J. Royal Stat. Soc. Ser. B* https://doi.org/10.1111/j.2517-6161.1995.tb02031.x (1995).
84. Lieberman, M. D. & Cunningham, W. A. Type I and type II error concerns in fMRI research: re-balancing the scale. *Soc. Cogn. Affect. Neurosci.* **4**, 423–428 (2009).
85. Winkler, A. M., Ridgway, G. R., Webster, M. A., Smith, S. M. & Nichols, T. E. Permutation inference for the general linear model. *Neuroimage* **92**, 381–397 (2014).
86. Faul, F., Erdfelder, E., Lang, A.-G. & Buchner, A. G*Power 3: a flexible statistical power analysis program for the social, behavioral, and biomedical sciences. *Behav. Res. Methods* **39**, 175–191 (2007).

Acknowledgements

Experiment 1 was financed by funding from the Secrétariat d'État à la formation, à la recherche et à l'innovation (SEFRI) to P.V. and O.K., under contract no. 15.0336 in the context of the European project 'Medit-Ageing'. The Age-Well randomized clinical trial (including experiment 2) is part of the Medit-Ageing project and is funded through the European Union's Horizon 2020 Research and Innovation Program (grant agreement no. 667696), Institut National de la Santé et de la Recherche Médicale, Région Normandie, and Fondation d'Entreprise MMA des Entrepreneurs du Futur to G.C., the project principal investigator (PI), and O.K., N.L.M., G.C. and A.L, work package leaders (co-PIs). Institut National de la Santé et de la Recherche Médicale (Inserm) is the sponsor. The funders and sponsor had no role in study design, data collection, and analysis, decision to publish or preparation of the manuscript. The authors are grateful to the Cyceron staff members for their help with neuroimaging data acquisition; as well as to the EUCLID team, the sponsor (H. Espérou, Pôle de recherche Clinique Inserm) and to all the participants in this study for their contribution. We acknowledge and thank the Medit-Ageing Research Group members for their contribution. We thank C. Bordas, S. de Cataldo and J. Sachs for their help on the mental thoughts analyses and their dedication during data acquisition. We also thank B. Bonnet and F. Grouiller as the principal staff members of the Brain and Behavior Laboratory in Geneva.

Author contributions

Conceptualization: S.B.L., O.K. and P.V.; data curation: S.B.L., Y.I.D.A., C.M., O.K. and P.V.; formal analysis: S.B.L. and Y.I.D.A.; funding acquisition: O.K., N.L.M., G.C., A.L. and P.V.; investigation: S.B.L., C.M. and members of the Medit-Ageing Research Group; methodology: S.B.L., Y.I.D.A., O.K., G.C. and P.V.; supervision: O.K. and P.V.; visualization: S.B.L.; writing—original draft: S.B.L.; writing—review and editing: S.B.L., A.L., F.C., G.C., N.L.M., O.K., P.V., C.M. and Y.I.D.A.

Competing interests

G.C. and A.L. reported personal fees from Fondation Entrepreneurs MMA and for G.C. from Fondation Alzheimer. The remaining authors declare no competing interests.

Additional information

Supplementary information The online version contains supplementary material available at https://doi.org/10.1038/s43587-022-00341-6.

Correspondence and requests for materials should be addressed to Sebastian Baez-Lugo, Patrik Vuilleumier or Olga Klimecki.

Peer review information *Nature Aging* thanks Mara Mather, Jaclyn Ford and the other, anonymous, reviewer(s) for their contribution to the peer review of this work.

Medit-Ageing Research Group

Eider Arenaza-Urquijo[6], Claire André[6], Sebastian Baez-Lugo[1,2], Maelle Botton[6], Pauline Cantou[6], Gaëlle Chételat[6], Anne Chocat[6], Fabienne Collette[3], Vincent De la Sayette[8], Marion Delarue[6], Stéphanie Egret[6], Eglantine Ferrand Devouge[6], Eric Frison[9], Julie Gonneaud[6], Marc Heidmann[4], Olga Klimecki[1,7], Elizabeth Kuhn[6], Brigitte Landeau[6], Gwendoline Le Du[6], Valérie Lefranc[6], Antoine Lutz[4], Natalie L. Marchant[5], Florence Mezenge[6], Inès Moulinet[6], Valentin Ourry[6], Géraldine Poisnel[6], Anne Quillard[6], Géraldine Rauchs[6], Stéphane Rehel[6], Clémence Tomadesso[6], Edelweiss Touron[6], Patrik Vuilleumier[1,2], Caitlin Ware[6] & Miranka Wirth[7]

[8]CHU Caen-Normandie, Department of Neurology, Caen, France. [9]EUCLID/F-CRIN Clinical Trials Platform, INSERM, CHU Bordeaux, University of Bordeaux, Bordeaux, France.

https://doi.org/10.1038/s43587-022-00341-6

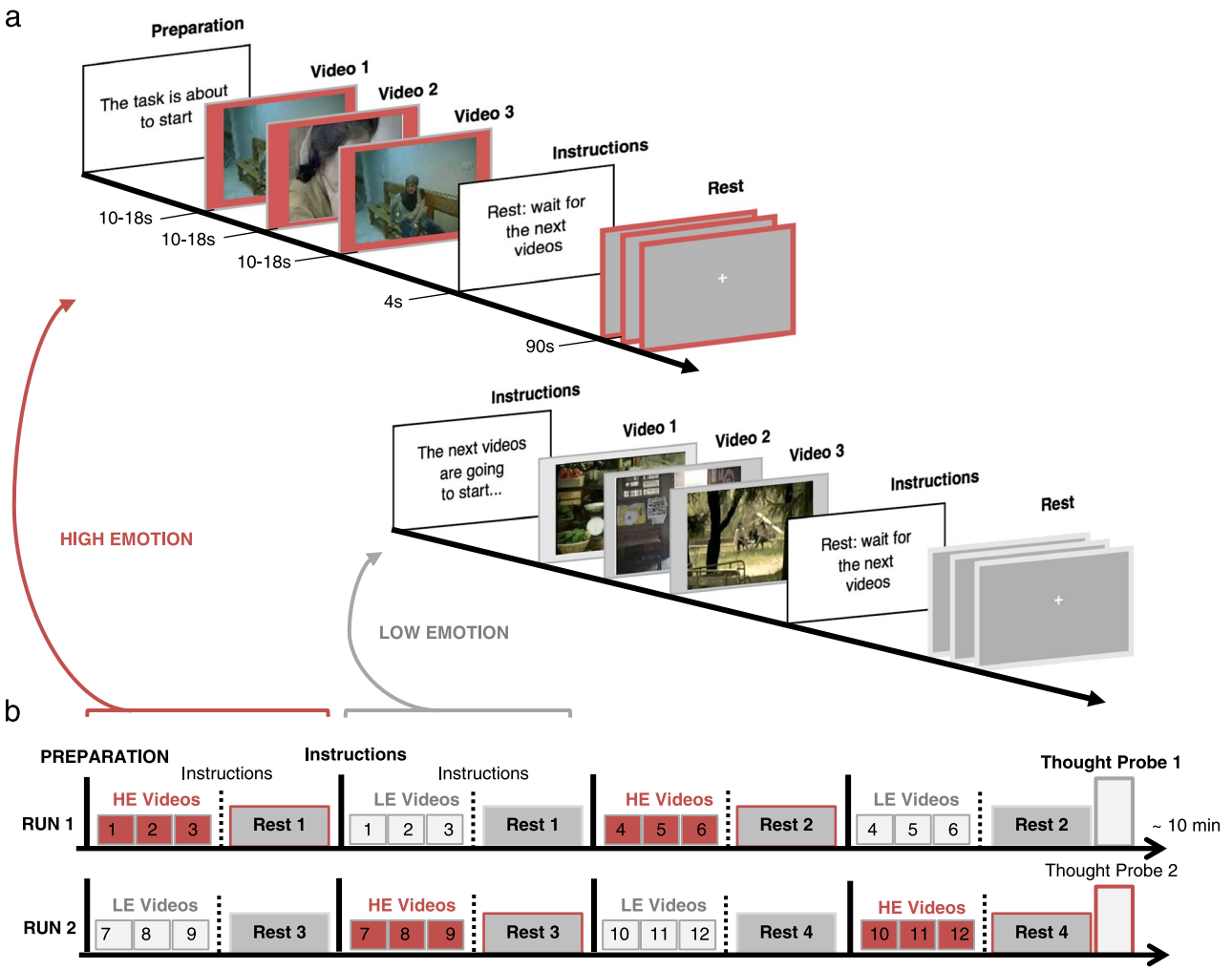

Extended Data Fig. 1 | Experimental design. (**a**) SoVT-Rest paradigm: 12 **High Emotion (HE)** and 12 **Low Emotion (LE)** videos were presented grouped in blocks of three. HE videos depict suffering people (for example, due to injuries or natural disasters), while LE videos depict people during everyday activities (for example, walking or talking). Each block of three videos is followed by a resting state period of 90 seconds. (**b**) Each run ends with a thought probe in which participants verbally express what they had been thinking and/or feeling during the last rest period (via a microphone), once following a LE block and once following a HE block. The order of the runs was randomized between participants. For further instructions regarding the SoVT-Rest task, please see Supplementary Table 2.

https://doi.org/10.1038/s43587-022-00341-6

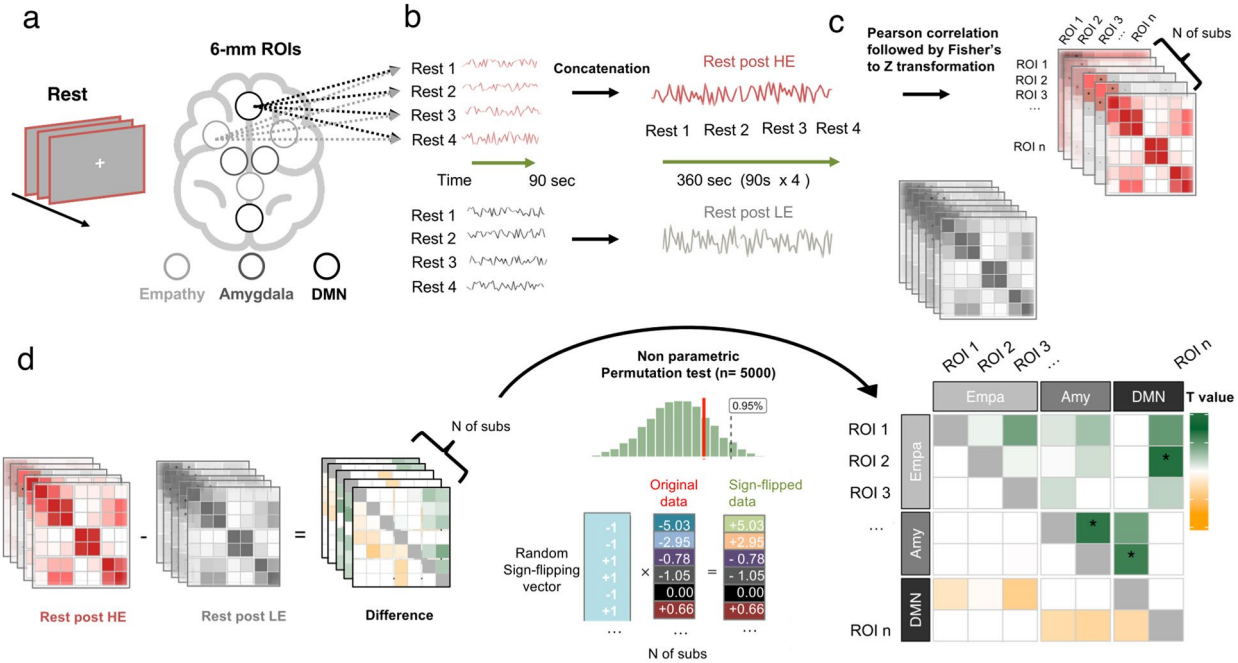

Extended Data Fig. 2 | Functional connectivity pipeline. (**a**) Regions of interest (ROIs) from the default mode network (DMN) were chosen based on Andrews-Hanna et al. (2010), including the posterior cingulate cortex (PCC, -8 -56 26) and anterior medial prefrontal cortex (aMPFC, -6 52 -2). ROIs from the empathy network (Empa) were based on the meta-analysis by Fan et al. (2011), including the bilateral anterior insula (AI, -36 16 2 and 38 24 -2) and anterior mid cingulate cortex (aMCC, -2 24 38). A 6 mm-radius sphere was created for each ROI. The amygdalae (Amy) were defined anatomically using the SPM anatomical template. (**b**) For every participant, time-series from the video and instruction periods were removed, and the remaining time-series corresponding to the rest periods were concatenated(Fair et al., 2007). The final concatenated time-series of the four rest blocks for each type of video (high emotion, HE or low emotion, LE) resulted in 184 frames (~360 s) of resting-state data for each subject. (**c**) We then correlated the time-courses between pairs of ROIs using Pearson's *r* correlation, and the resulting coefficients were Fisher's *r* to *z* transformed to improve normality in the data. Individual *Z*-score maps (correlation matrices) were created for each participant. (**d**) Significant differences between the two correlation matrices (post-HE vs. post-LE Rest) were tested using a non-parametric permutation test(Winkler et al., 2014). For each pair of nodes, the permutation test compared the true correlation difference t_{real} (HE vs. LE) to a null distribution $t_{permuted}$ constructed by randomly flipping the sign of the correlation coefficients and repeating the *t* statistic ($n = 5000$).

Corresponding author(s): Sebastian Baez Lugo
Patrik Vuilleumier
Olga Klimecki

Last updated by author(s): Nov 24, 2022

Reporting Summary

Nature Portfolio wishes to improve the reproducibility of the work that we publish. This form provides structure for consistency and transparency in reporting. For further information on Nature Portfolio policies, see our Editorial Policies and the Editorial Policy Checklist.

Statistics

For all statistical analyses, confirm that the following items are present in the figure legend, table legend, main text, or Methods section.

n/a	Confirmed
☐	☒ The exact sample size (*n*) for each experimental group/condition, given as a discrete number and unit of measurement
☐	☒ A statement on whether measurements were taken from distinct samples or whether the same sample was measured repeatedly
☐	☒ The statistical test(s) used AND whether they are one- or two-sided *Only common tests should be described solely by name; describe more complex techniques in the Methods section.*
☐	☒ A description of all covariates tested
☐	☒ A description of any assumptions or corrections, such as tests of normality and adjustment for multiple comparisons
☐	☒ A full description of the statistical parameters including central tendency (e.g. means) or other basic estimates (e.g. regression coefficient) AND variation (e.g. standard deviation) or associated estimates of uncertainty (e.g. confidence intervals)
☐	☒ For null hypothesis testing, the test statistic (e.g. *F*, *t*, *r*) with confidence intervals, effect sizes, degrees of freedom and *P* value noted *Give P values as exact values whenever suitable.*
☒	☐ For Bayesian analysis, information on the choice of priors and Markov chain Monte Carlo settings
☒	☐ For hierarchical and complex designs, identification of the appropriate level for tests and full reporting of outcomes
☐	☒ Estimates of effect sizes (e.g. Cohen's *d*, Pearson's *r*), indicating how they were calculated

Our web collection on statistics for biologists contains articles on many of the points above.

Software and code

Policy information about availability of computer code

Data collection	Matlab 2012 + Cogent 2000 Toolbox
Data analysis	Matlab 2017 + SPM version 12, fsl_regfilt function of FSL (version 6.0). R studio (version 3.6.1), ggplot2 (version 3.2.1).

For manuscripts utilizing custom algorithms or software that are central to the research but not yet described in published literature, software must be made available to editors and reviewers. We strongly encourage code deposition in a community repository (e.g. GitHub). See the Nature Portfolio guidelines for submitting code & software for further information.

Data

Policy information about availability of data

All manuscripts must include a data availability statement. This statement should provide the following information, where applicable:

- Accession codes, unique identifiers, or web links for publicly available datasets
- A description of any restrictions on data availability
- For clinical datasets or third party data, please ensure that the statement adheres to our policy

The data underlying this report are made available on request following a formal data sharing agreement and approval by the consortium and executive committee (https://silversantestudy.eu/2020/09/25/data-sharing). The Material can be mobilized, under the conditions and modalities defined in the Medit-Ageing Charter, by any research team belonging to an Academic for carrying out a scientific research project relating to the scientific theme of mental health and well-being in older people. The Material may also be mobilized by non-academic third parties, under conditions, in particular financial, which will be established by separate agreement between Inserm and by the said third party. Data sharing policies described in the Medit-Ageing Charter are in compliance with our ethics approval and guidelines from our funding body.

Field-specific reporting

Please select the one below that is the best fit for your research. If you are not sure, read the appropriate sections before making your selection.

☐ Life sciences ☒ Behavioural & social sciences ☐ Ecological, evolutionary & environmental sciences

For a reference copy of the document with all sections, see nature.com/documents/nr-reporting-summary-flat.pdf

Behavioural & social sciences study design

All studies must disclose on these points even when the disclosure is negative.

Study description	This is a quantitative cross-sectional fMRI study on socio-emotional processing in younger and older adults. The data presented is from the baseline visit of the Age-Well randomized clinical trial within the Medit-Ageing Project.
Research sample	The present study comprises behavioral and neuroimaging measures from two independent experiments with a total sample of n=182 participants with corrected-to-normal vision and no history of neurological or psychiatric disorders. Experiment 1 was conducted with a total of 55 healthy participants including 29 young participants (M age= 24, 14 females) and 26 older participants (M age = 68.7, 13 females). Experiment 2 was conducted with a total of 127 community-dwelling older adult participants (M age = 68.8 years, SD = 3.63, 79 females); this sample was part of the baseline visit of the Age-Well randomized clinical trial within the Medit-Ageing Project .
Sampling strategy	For Experiment 1, no statistical methods were used to pre-determine sample sizes but our sample sizes are similar to those reported in previous publications(Chen et al., 2014; Eryilmaz et al., 2011). For the Age-well RCT (which includes Experiment 2 data), an effect size of 0.75 per comparison was targeted, with 80% power and a two-sided type I error of 1.25% (Bonferroni correction for test multiplicity), resulting in a total of 126 participants needing to be included. The final number of participants in the Age-Well RCT(n=137) was higher than the required minimum of 126(Chételat et al., 2022; Poisnel et al., 2018). Sensitivity analyses then indicated that the final sample included in Experiment 2 (n=127) was reliable and sensitive enough to detect small-to-medium-sized effects at a voxel level (α = 0.001, dz = 0.37), given a power of 1-ß = 0.8(Faul et al., 2007).
Data collection	The neuroimaging data collection took place in a at the Brain and Behavior Laboratory of the University of Geneva, using a 3T whole-body MRI scanner (Trio TIM, Siemens, Germany) with the 32-channel head coil (Experiment 1); and at the GIP Cyceron (Caen, France) using a Philips Achieva (Eindhoven, The Netherlands) 3T scanner with a 32-channel head coil(Experiment 2). The behavioral data was collected via computer as well as pen and paper. MRI technicians and one or two researchers were always present inside the room during data collection. Our analyses do not require to use blinding techniques given that all participants performed to all conditions. The data from Experiment 2 was part of a clinical trial but the current article assess baseline measurements before they were allocated to any experimental group.
Timing	Data collection started in December 2016 and ended in February 2021.
Data exclusions	In Experiment 1 , n=3 participants were excluded due to a priori exclusion criteria including artifacts in brain images and/or extreme head motion during scanning. In Experiment 2, two participants were excluded for eligibility criteria and intervention allocation issues(Chételat et al., 2022). N=8 participants were excluded from the final data analysis due to a priori exclusion criteria: abnormal brain morphology (n = 3), extreme head motion (n = 3), and presence of artifacts in brain images (n = 2).
Non-participation	All recruited participants completed the experiment.
Randomization	For both experiments, the video sets (V1, V2, and V3) and whether participants started the experiment with HE or LE videos first were randomly attributed to participants in an excel table. While investigators were blinded to the training arm that participants were randomized to in the Age-Well trial, no blinding was performed for the SoVT-Rest task at baseline (Experiment 2).

Reporting for specific materials, systems and methods

We require information from authors about some types of materials, experimental systems and methods used in many studies. Here, indicate whether each material, system or method listed is relevant to your study. If you are not sure if a list item applies to your research, read the appropriate section before selecting a response.

Materials & experimental systems

n/a	Involved in the study
☒	☐ Antibodies
☒	☐ Eukaryotic cell lines
☒	☐ Palaeontology and archaeology
☒	☐ Animals and other organisms
☐	☒ Human research participants
☐	☒ Clinical data
☒	☐ Dual use research of concern

Methods

n/a	Involved in the study
☒	☐ ChIP-seq
☒	☐ Flow cytometry
☐	☒ MRI-based neuroimaging

Human research participants

Policy information about studies involving human research participants

Population characteristics	The present study comprises behavioral and neuroimaging measures from two independent experiments with a total sample of n=182 participants with corrected-to-normal vision and no history of neurological or psychiatric disorders. Experiment 1 was conducted with a total of 55 healthy participants including 29 young participants (M age= 24, 14 females) and 26 older participants (M age = 68.7, 13 females). Experiment 2 was conducted with a total of 127 participants (M age = 68.8 years, SD = 3.63, 79 females); this sample was part of the baseline visit of the Age-Well randomized clinical trial within the Medit-Ageing Project .
Recruitment	Participants were recruited via advertising in media outlets, social media, and flyers distributed in relevant local events, places and universities in Geneva (Switzerland) and Caen (France). The Age-Well trial involved a commitment to 18 months of training and repeated measurements. Most likely, only participants highly motivated to contribute to research took part in the study. This is confirmed by the extremely low attrition in Age-Well: no participant discontinued the study in 18 months. The only drop-outs were due to death.
Ethics oversight	Experiment 1 was approved by the local Swiss ethics committee (commission cantonale d'éthique de la recherche CCRE, Geneva, Switzerland) under the project number 2018-01980. The Age-Well randomized clinical trial (Experiment2) was approved by the ethics committee (Comité de Protection des Personnes Nord-Ouest III, Caen, France; trial registration number: EudraCT: 2016-002441-36; IDRCB: 2016-A01767-44; ClinicalTrials.gov Identifier: NCT02977819).

Note that full information on the approval of the study protocol must also be provided in the manuscript.

Clinical data

Policy information about clinical studies

All manuscripts should comply with the ICMJE guidelines for publication of clinical research and a completed CONSORT checklist must be included with all submissions.

Clinical trial registration	ClinicalTrials.gov Identifier: NCT02977819
Study protocol	Part of the data presented in this study (Experiment 2) is part of the baseline of the randomized clinical trial AGE-WELL. For the full trial study protocol please see Poisnel et al.,2018
Data collection	data from the Age-Well randomized clinical trial of the Medit-Ageing European project was acquired between 2016 and 2018 at Cyceron Center in Caen, France.
Outcomes	This study comprises part of the secondary outcomes of the randomized clinical trial AGE-WELL. For the full trial outcomes please see Poisnel et al.,2019

Magnetic resonance imaging

Experimental design

Design type	Block design
Design specifications	During the task, participants watch 12 High Emotion (HE) and 12 Low Emotion (LE) video-clips grouped in blocks of three. Each block was followed by a resting state period of 90 seconds. The experimental design consisted in two sessions. Each session included the fixation cross (10 sec), instructions (4 sec/8 sec), three videos (~15 seconds each) modelled separately, and rest periods following each block (90 sec). Each rest period was divided into three equal parts (30-seconds time bins). The total duration of the SoVT-Rest fMRI paradigm was approximately 21 minutes, consisting of 9.5 min for each session plus 1 minute on average for each thought probe.
Behavioral performance measures	After the fMRI session, participants watched all video clips again on a computer outside the scanner and provided ratings on their subjective experience of empathy, positive affect and negative affect state, for each of the 24 videos.

Acquisition

Imaging type(s): Structural and functional magnetic resonance imaging (MRI, fMRI)

Field strength: 3 Tesla

Sequence & imaging parameters: For Experiment 1, A high-resolution T1-weighted anatomical volume was first acquired using a magnetization-prepared rapid acquisition gradient echo (MPRAGE) sequence (repetition time = 1900 ms; echo time = 2.27 ms; flip angle = 9°; slice thickness = 1 mm; field of view = 256x256 mm2; in plane resolution = 1x1 mm2). Blood oxygen level-dependent (BOLD) images were acquired with a susceptibility weighted EPI sequence (TR/TE =2000/30 ms, flip angle = 85°, voxel size (3 x 3 mm), 35 slices, 3 mm slice thickness, 20% slice gap, direction of acquisition = descending). For Experiment 2, a high-resolution T1-weighted anatomical volume was first acquired using a 3D fast field echo sequence (3D-T1-FFE sagittal; repetition time = 7.1 ms; echo time = 3.3 ms; flip angle = 6°; 180 slices with no gap; slice thickness = 1 mm; field of view = 256x256 mm2; in plane resolution = 1x1 mm2). Blood oxygen level dependent (BOLD) images were acquired during the SoVT-Rest task with a T2*-weighted asymmetric spin-echo echo-planar sequence (each run ~10.5 min; TR = 2000 ms, TE = 30 ms, flip angle = 85°, FOV = 240 x 240 mm2, matrix size = 80 x 68 x 33, voxel size = 3 × 3× 3 mm3, slice gap = 0.6 mm) in the axial plane parallel to the anterior–posterior commissure.

Area of acquisition: Whole brain scan was used

Diffusion MRI ☐ Used ☒ Not used

Preprocessing

Preprocessing software: In Experiment 1, the preprocessing included the following steps: 1) EPI data were realigned to the first volume and spatially smoothed with an 8-mm FWHM Gaussian kernel. 2) Preprocessed fMRI data were denoised for secondary head motion and CSF-related artifacts using automatic noise selection as implemented in ICA-AROMA, a method for distinguishing noise-related components based on ICA decomposition. Additionally, components with high spatial overlap with white matter regions were also removed by means of a linear regression using the fsl_regfilt function of FSL (FMRIB's Software Library, www.fmrib.ox.ac.uk/fsl). 3) Denoised EPI data were coregistered to the anatomical T1 volume. 4) The anatomical T1 volume was segmented and the extracted parameters were used to 5) normalize all EPIs volumes into the Montreal Neurological Institute (MNI) space. This procedure was performed using FSL and SPM12. In Experiment 2, the preprocessing was conducted using Statistical Parametric Mapping software (SPM12) implemented on Matlab 2017 and followed a methodology designed to reduce geometric distortion effects induced by the magnetic field, described by Villain and colleagues (2010). This procedure included the following steps: 1) realignment of the EPI volumes to the first volume and creation of the mean EPI volume, 2) coregistration of the mean EPI volume and anatomical T1, T2, and T2* volumes, 3) warping of the mean EPI volume to match the anatomical T2* volume, and application of the deformation parameters to all the EPI volumes, 4) segmentation of the anatomical T1 volume, 5) normalization of all the EPIs, T1 and T2* volumes into the Montreal Neurological Institute (MNI) space using the parameters obtained during the T1 segmentation, 6) 8 mm FWHM smoothing of the EPI volumes.

Normalization: See above.

Normalization template: The volumes were normalized into the Montreal Neurological Institute (MNI) space provided by SPM12.

Noise and artifact removal: Six rigid-body realignment parameters in addition to censored volumes using frame-wise displacement (FD) were included as nuissance covariates when estimating the 1st-level statistical maps.

Volume censoring: We performed data censoring as described by Power and colleagues (2012). During the estimation of beta coefficients for each regressor of interest, volumes with frame-wise displacement (FD) >0.5 mm were flagged in the design matrices and ignored during the estimation of the 1st -levels.

Statistical modeling & inference

Model type and settings: For the fist-level, the different regressors were convolved with a hemodynamic response function (HRF) according to a block design for univariate regression analysis. Low-frequency drifts were removed via a high-pass filter (cutoff frequency at 1/ 256 Hz). For the 2nd-level analysis, we used a flexible factorial design where the estimated parameters from 1st-level contrasts of interest were entered separately for each subject. These analyses were generated with SPM12.

Effect(s) tested: We used a factorial design to investigate the effect of each experimental condition on brain activity, including the main condition effects (video and rest) as well as the specific emotional effects (HE and LE) during either the video or the subsequent rest periods. We then conducted T-tests contrasts to compare the conditions of interest (videos vs. rest periods and vice versa), the specific emotional effects (videos: HE vs. LE; rest: HE vs LE) as well as between-group differences (Young vs. Old)

Specify type of analysis: ☐ Whole brain ☐ ROI-based ☒ Both

Anatomical location(s): For the functional connectivity analyses, the selected a priori ROIs for the default mode network (DMN) and the Empathy newtwork were determined based on results from previous relevant studies and meta-analyses (Andrews-Hanna et al., 2010 and Fan et al., 2011). The amygdala was defined anatomically using the current SPM anatomical template provided by Neuromorphometrics, Inc (http://Neuromorphometrics.com/).

Statistic type for inference
(See Eklund et al. 2016)

We used voxel-wise and cluster-wise inference corrected for multiple comparisons. For completeness, in Experiment 1 we additionnaly report some fMRI results at whole-brain P uncorrected < 0.001, k > 20 which has been shown to be acceptable and reliable for fMRI experiments assessing cognitive and affective processes with unprecise onsets (Lieberman, 2009).

Correction

Comparisons are reported with a whole-brain family-wise error (FWE) correction at p < 0.05, at the voxel and cluster level.

Models & analysis

n/a	Involved in the study
☐	☒ Functional and/or effective connectivity
☒	☐ Graph analysis
☒	☐ Multivariate modeling or predictive analysis

Functional and/or effective connectivity

Functional connectivity analyses were performed using Matlab 2017 and R studio (version 3.6.1). For each participant, time courses of activity (from each voxel of the brain) were high-pass filtered at 256 Hz, detrended and standardized (Z-score), before extracting specific time courses from the defined ROIs. Nuisance regressors included white matter (WM) and cerebrospinal fluid (CSF) signals, and the realignment parameters. For each participant, time-series from the instructions and videos periods were removed, and the remaining time series corresponding to the rest periods were concatenated. We then correlated the time-courses between the different ROIs using Pearson correlations and the resulting coefficients were Fisher's r to z transformed. Individual Z-score maps (correlation matrices) were created for each participant. To test for significant differences between the two correlation matrices (post HE rest and post LE rest), we used a non-parametric permutation test.